# Modeling, Performance Analysis, and Optimization of Erbium-Doped Optical Amplifier

*By*

**Rana Ahmad Ramadan**

*Supervisor*

**Dr. Ibrahim Mansour**

**Submitted in Partial Fulfillment of Requirements for the Degree of Master of Science in**
Electrical Engineering/ Communications

Faculty of Graduate studies
University of Jordan

May, 2000

This thesis was successfully defended and approved on Monday, 22/5/2000

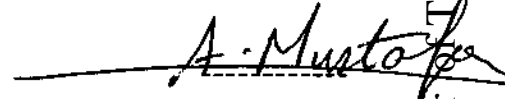Examination committee                                    Signature

Dr. Ibrahim Mansour, chairman
Assist. Prof. In Communications

Dr. Ahmad Mustafa, member
Assist. Prof. In Communications

Dr. Jamal Rahhal, member
Assist. Prof. In Communications

Prof. Mansour Al-Abbadi, member
Prof. In Communications

# Dedication

*To those two who give meaning to my life*
*and stand by me in times of hardship and gloaming*
*To you my dear parents.*

# Acknowledgements

I sincerely thank my supervisor, Dr. Ibrahim Mansour whose help and suggestions were valuable in preparing this work. Also I wish to acknowledge the support my friends; here and aboard. My sincere appreciation is extended to all those friends, family members who stimulated thoughts and initiation through out this work.

# List of Contents

# List of Figures

# Abstract

## Modeling, performance analysis, and optimization of Erbium-doped Optical Amplifier

by

**Rana Ahmad Ramadan**

Supervisor

**Dr. Ibrahim Mansour**

Nowadays, optical communication systems are widely used specially in the high bit rate. In these systems optical amplifiers are used to replace conventional electronic repeaters due to the fact that electronic repeaters can not operate in these ranges and to other attractive features (optical amplifiers are transparent to bit rate and operating wavelength).

The excellent properties of Erbium Doped Optical Amplifiers and their use in optical telecommunication systems have encouraged many researchers to work on optimizing their performance.

In this work, a theoretical framework for optical amplification mechanism in $Er^{3+}$-doped waveguides has been developed, then a numerical model is obtained to evaluate the amplifier performance as function of manufacturing parameters and operating conditions; such as the absorption and emission cross sections, the erbium concentration profile, and the mode intensity distribution.

Moreover, different amplifier parameters are studied to advise best geometrical and manufacturing variables that produce maximum gain and optimize the amplifier performance.

# CHAPTER (1):INTRODUCTION

## 1.1 Advantages of Optical Fiber Communication

There are several advantages for using optical fibers as transmission media. Many of these result from the fact that the principal material in fiber manufacture is glass. Hence it is useful to consider the merits and special features offered by the optical fiber communications over those conventional electrical communications.

*(a) Enormous potential bandwidth.* The optical carrier frequency in the near infrared around $10^{14}$ Hz or $10^5$ GHz, yields a far greater potential transmission bandwidth than coaxial cable or even radio wave systems. At present, the bandwidth available to fiber systems is not fully utilized but modulation at several gigahertz over a hundred kilometers and hundreds of megahertz over three hundred kilometers without repeaters is possible. Also using wavelength division multiplexing WDM, allows enhancing bandwidth utilization for an optical fiber, by transmitting several optical signals.

*(b) Small size and weight.* Optical fibers have very small diameters which are often no greater than the diameter of a human hair. This encourages using them in aircraft, satellite, and in crowded ducts under city streets.

*(c) Electrical isolation.* A further advantage of glass is that it is non-conductive; the fiber thus creates no arcing or spark hazard at short circuits. **520324**

*(d) Immunity to interference and crosstalk.* Due also to glass dielectricity , the fiber forms a transmission channel that is essentially immune to most forms of external electromagnetic interference. (Buck,1995). The fiber cable is also not susceptible to lightning strikes if used overhead rather than underground. Moreover, it is fairly easy to ensure that there is no optical interference between fibers, and hence crosstalk is negligible.

*(e) Signal security.* The light from optical fibers does not radiate significantly and therefore they provide a high degree of signal security. This feature is obviously attractive for military, banking and general data transmission applications.

*(f) Low transmission loss.* The development of optical fibers over the last twenty years has resulted in the production of optical fiber which exhibit very low attenuation or transmission loss in comparison with the best copper conductors. Fibers have been fabricated with losses as low as 0.2 dB/km, and this feature has become a major advantage of optical fiber communications. It facilitates the implementation of communication links with widely separated repeaters.

*(g) Ruggedness and flexibility.* Although protective coatings are essential, optical fibers may be manufactured with very high tensile strengths. The fibers may also be bent to quite small radii or twisted without damage.

*(h) System reliability and ease of maintenance.* These features primarily stem from the low loss property of optical fiber cables which reduces the requirement for intermediate repeaters or line amplifiers to boost the transmitted signal strength. Hence with fewer repeaters, system reliability is generally enhanced in comparison with conventional electrical conductor systems. Furthermore, the reliability of the optical components is no longer a problem with predicted lifetimes of 20 to 30 years now quite common. Both these factors also tend to reduce maintenance time and costs.

*(i) Potential low cost.* The glass which generally provides the optical fiber transmission medium is made from sand- not a scarce resource. So, in comparison with copper conductors, optical fibers offer the potential for low cost line communication. Although it is not the case for the other component associated with optical fiber communications, for example, semiconductors lasers, couplers, connectors, etc. Overall

system costs when utilizing optical fiber communication on long-haul links, however, are substantially less than those for equivalent electric line systems.

## 1.2 Five Generation of Lightwave Systems

Figure (1.1) shows the progress in the performance of lightwave systems realized through several generations of development.
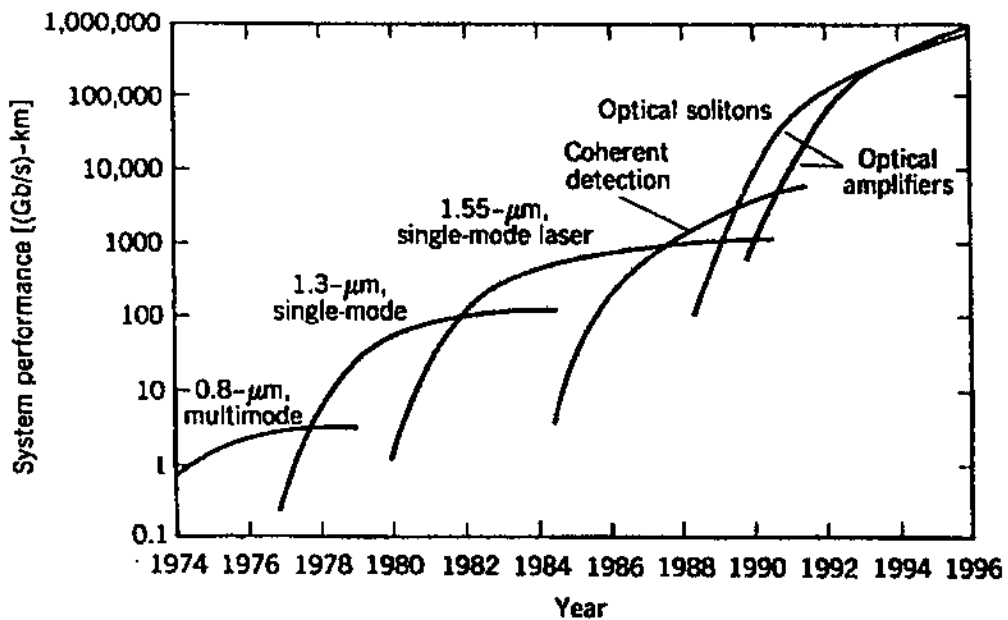


Figure 1.1: Progress in lightwave communication technology over period 1974-1996

*The first generation* lightwave systems operating near 0.8μm became available commercially in 1980 (Agrwal,1997). They operated at a bit rate of 45Mb/s and allowed a repeater spacing of about 10km, which considered large spacing compared to that of a coaxial system.

*The second generation* 1.3 μm lightwave systems operating at bit rate of up to 1.7 Gb/s with a repeater spacing of about 50km, were commercially available by 1987 (Agrawal,1997). Operating in the wavelength region near 1.3 μm, where fiber loss is below 1 dB/km. Furthermore, optical fibers exhibit minimum dispersion in this

wavelength region. Bit rate limit had been overcome by introducing single-mode fibers instead of multimode fibers.

*Third-generation* 1.55 μm systems operating at a bit rate up to 10 Gb/s became available commercially in the early 1990s .The loss of silica fibers is minimum near 1.55 μm (typically, 0.2 dB/km), but the large fiber dispersion near this wavelength prevented the third-generation from quick realization. The dispersion problem can be overcome either by using dispersion-shifted fibers designed to have minimum dispersion near 1.55 μm or by limiting the laser spectrum to a single longitudinal mode, and the best performance is achieved by using both.

It may be suitable here to briefly talk about dispersion. Different light components (different modes and/or different frequency or colors) travel through the fiber at generally different velocities causing dispersion. When a composite optical signal travels through the fiber, it can be distorted due to fiber dispersion. Usually dispersion occurs due to two reasons:

- The silica dielectric constant, ε, and therefore, the refractive index, n, depends on the light frequency, ω, this is called material dispersion.

- The propagation constant, β, depends on the light frequency,ω, in a nonlinear fashion even if,ε, were independent of, ω, this is known as wavelength dispersion. The wavelength is known as the zero-dispersion wavelength if the total material dispersion and waveguide dispersion equal to zero at this wavelength. Using conventional fiber, zero-dispersion occurs at 1.3 μm. Using dispersion-shifted fibers, zero-dispersion occurs at 1.55 μm.

*The fourth generation* of lightwave systems makes use of optical amplification for increasing the repeater spacing and of Wavelength Division Multiplexing (WDM) for increasing the bit rate. In such systems fiber loss is compensated periodically using erbium-doped fiber amplifiers spaced 60-100 km apart. Such systems became available commercially by 1990.

The current emphasis of fourth-generation is on increasing the system capacity by transmitted multiple channels though the WDM technique. Optical amplifiers are ideal for multichannel lightwave systems since all channels can be amplified simultaneously without requiring demultiplexing transmitted over 9100 km in a recirculating loop configuration (Agrawal,1997), resulting in a total bit rate of 100 Gb/s. In another record experiments, a total bit rate of 1.1 Tb/s was achieved by multiplexing 55 channels, each operating at 20Gb/s. Despite the use of dispersion compensation schemes, dispersive effects limited the total transmission distance to 150km. Commercially WDM systems operating at a bit rate of up to 40 Gb/s were available by the end of 1996 (Agrawal,1997).

*The fifth generation* of fiber-optic communication systems is concerned with finding a solution to the fiber-dispersion problem. Optical amplifiers solve the loss problem but, at the same time, make the dispersion problem worse since the dispersive effects accumulate over multiple amplification stages, the proposed solution is the soliton. The Solitons are optical pulses that preserve their shape during propagation in a lossless fiber by counteracting the effect of dispersion through the fiber nonlinearity. (Agrawal,1997).

## 1.3 Literature Survey and Contribution

Erbium Doped Fiber Amplifiers were modeled using the propagation and rate equations of a homogenous, two-level laser medium. Numerical methods were used to calculate the gain and ASE spectra. Also the effects of multimode pumping were analyzed. The researchers also compared the performance of 1480nm and 980nm pumped amplifiers, and optimized fiber design for high pump efficiency (Giles and Desurvire, 1991).

An accurate model for Erbium Doped Fiber Amplifier was presented. The model was used to design the index profile of the doped fiber, optimizing with regard to efficiency. The predicted pump efficiency were also compared to experimental results and gave very good agreement (Pedersen, at al., 1991).

The amplification characteristics of gain-flattened $Er^{3+}$-doped fiber amplifiers were studied (Ono, at al.,1999), it was shown there that the flattened amplification bandwidth was 1570-1600 nm for silica-based fibers, and 1565-1600 nm for fluoride-based fibers. Moreover, it was shown there that pumping at 1480 nm has a better conversion efficiency and gain coefficient than that for pumping at 980nm.

In this work, the same mathematical model as that used by Pedersen, et al., was used. Taking into consideration almost all the design parameters affecting the performance of Erbium Doped Fiber Amplifiers, all optimized for the maximum gain, since pump efficiencies are not always the best criteria to use in designing an Erbium Doped Fiber Amplifier.

The effects of signal wavelengths and the initial signal power were also investigated. The saturation power was also calculated for different initial pump power.

The simple numerical method suggested was reliable to obtain accurate results, with a reasonable computational time.

# 1.4 Optical Amplifiers

Electronic repeaters (regenerators) were used to strengthen the propagating signal within the optical system. These regenerators require optical-electrical and electrical-optical conversion devices which cause a considerable limitation in the implementation of optical fiber systems. The conversion of the information signal from the electrical domain to the optical domain and visa-versa often provides a bottleneck within optical fiber communications, which may restrict both the operating bandwidth and the quality of the transmitted signal. Performing operations on signals in the optical domain significantly increased within optical fiber communications and its associated application areas (Senior,1992).

Optical amplifiers, as their name implies, operate solely in the optical domain with no interconversion of photons to electrons. They are ideally a transparent box that provides gain and is also insensitive to the bit-rate, modulation format, power, and wavelengths of signals passing through it (Kazovsky, et al., 1996). See Figure (1.2) below:
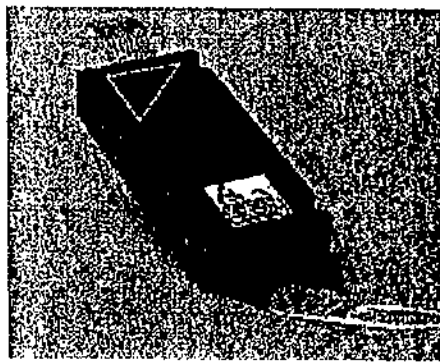


**Figure 1.2: Commercially available EDFA**

The signals remain in optical form during amplification. And optical amplifiers are potentially cheaper and more reliable than regenerators. Moreover, optical amplifier can be bidirectional and allow multiplex operation of several signals at

different optical wavelengths (i.e. Wave Division Multiplexing). Provided that for long-haul systems; (1) the signal wavelength must be near 1.55 μm for lowest attenuation, and (2) the fiber must be dispersion-shifted, with its dispersion parameter having a value close to zero at the signal wavelength.

## 1.4.1 Basic Amplifier Configuration

Figure (1.3) shows different configurations used in applying optical amplifiers to optical communications systems. Optical amplifiers are used as post-amplifiers at the optical transmitter for increasing the light level, in-line amplifiers are used along the optical fiber transmission path, and pre-amplifiers are used at the optical receiver for improving its sensitivity. In the signal distribution system shown in Figure (1.3 c), the optical amplifiers serve as booster amplifiers which compensate for optical branching losses by amplifying the optical output level.

Next, a brief comparison for the different properties requirement of optical amplifiers in various applications:

- *Post amplifier*: It is placed immediately following the laser transmitter. Used to increase the transmission distance of point-to-point fiber links by raising the signal power so the signal is still above the thermal noise level of the receiver even after attenuation. This type of optical amplifiers handles high optical input levels, typically (0.1-1.0mW), the key parameter here will be to maximize the saturation output power (the optical output at which the gain falls by 3dB). This was tested for a signal of 2.5Gb/s that was transmitted over 318km in 1992. (Agrawal,1997).
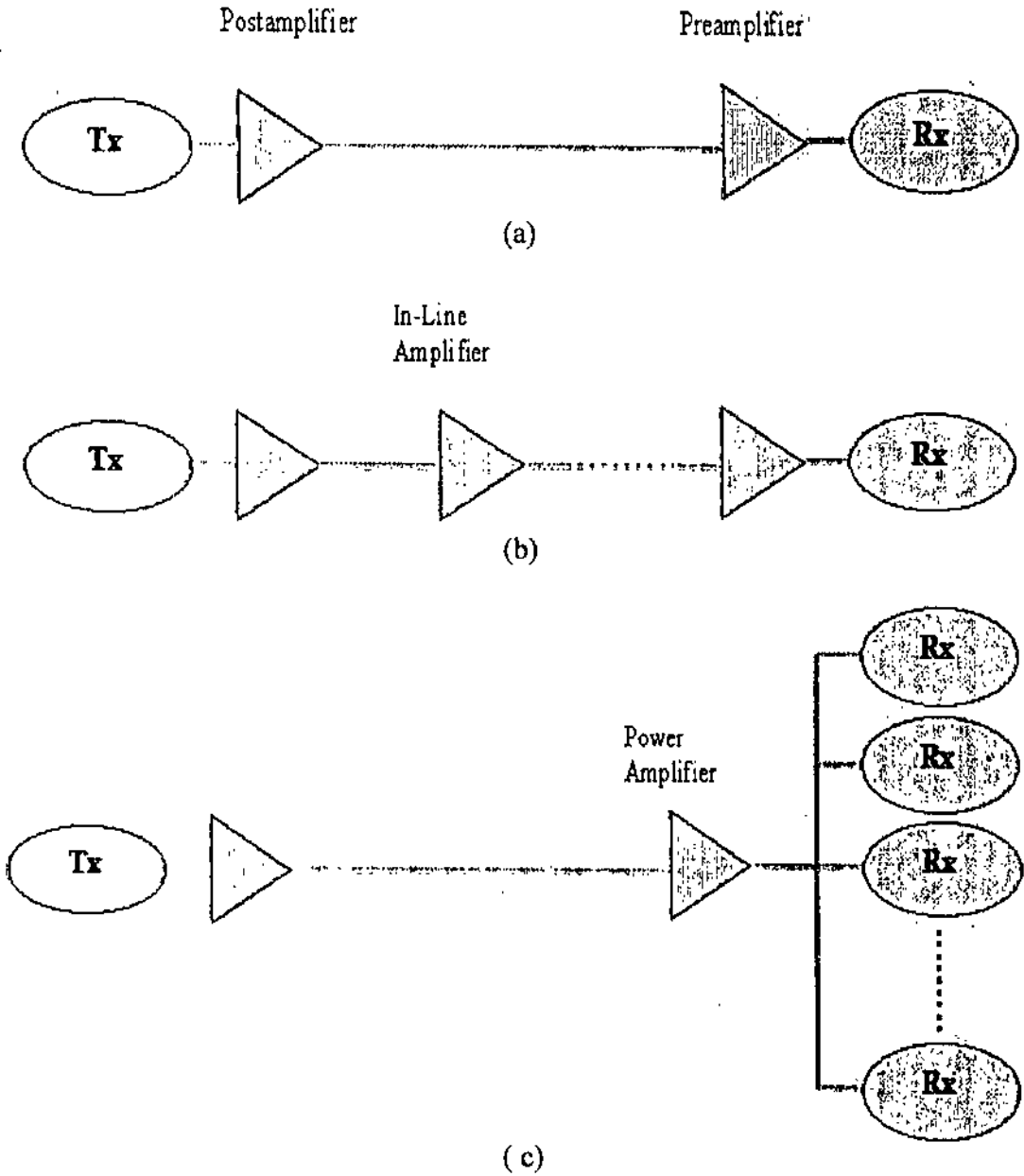
Figure 1.3: Three types of transmission systems with fiber amplifier: (a) a postamplifier and a preamplifier, (b) a transmission system with fiber amplifier repeaters, (c) an information distribution system using power amplifier

- *The preamplifier*: It is placed directly before the receiver, where the signal has already been significantly attenuated along the transmission path. Its main purpose is to make the optical signal strong enough such that the thermal noise becomes

negligible compared to the shot noise. As a result, the receiver sensitivity can be improved. The main Figures of merit are high gain and low amplifier noise. In a 1990 experiment, a receiver sensitivity of -37.2dBm was achieved at high bit rate of 10Gb/s using one EDFA (Agrawal,1997).

- *The in-line amplifier*: It is placed in-line and perhaps incorporated at one or more places along the transmission path. The amplifier corrects for periodic signal attenuation due either to fiber absorption or to network distribution-splitting losses. The performance demanded for this type of amplifier depends on the intended repeater number and transmission speed; essentially it should have high gain, and low noise characteristics. It is mainly used in applications where transmission distances in excess of 300km. In 1996 experiment the 10Gb/s signal was transmitted over 442km using two remotely pumped in-line amplifiers.

- *Booster Amplifier*: Figure (1.3 c) shows an information distribution system that uses fiber amplifier as a power amplifier. Here the visual signals are amplified before being distributed to several arms. High saturation output and high gain are the most essential characteristics for such an amplifier. It is suitable for LANs such as fiber-to-the-home systems. The system tested in 1990 was capable of transmitting the composite video signal to 0.52 million subscribers. In another experiment the broadcast network was capable to transmitting 35 video channels to 4.2 million subscribers. (Agrawal,1997).

## 1.4.2 Types of Optical Amplifiers

The most popular types of optical amplifiers were developed; Semiconductor optical amplifiers (SOAs) and Erbium-doped fiber optic amplifiers (EDFAs), both consists of active medium that has its carriers inverted into an excited energy level, thus enabling an externally input optical field to initiate stimulated emission and achieve coherent gain. The population inversion is achieved by the absorption of energy from a pump source, and an external signal must be efficiently coupled into and out of the amplifier. Figure (1.4) depicts the basic amplifier building blocks for an SOA and an EDFA.

An SOA is nothing more than a semiconductor laser, with or without facet reflections (the antireflection coating reduces the reflections). An electric current inverts the medium band, thereby producing spontaneous emission (fluorescence) and the potential for stimulated emission if an external optical field is present. The stimulated emission yields the signal gain. On the other hand, the spontaneous is itself amplified and considered the randomly fluctuating amplifier noise, called the amplified spontaneous emission (ASE).

The fiber amplifier is a length of glass fiber that has been doped with ions of a rate-earth metal, such as erbium. The ions act as an active medium with the potential to experience inversion of carriers and emit spontaneous and stimulated emission light near a desirable signal wavelength. The pump typically is another light source whose wavelength is preferentially absorbed by ions.

(a)



(b)
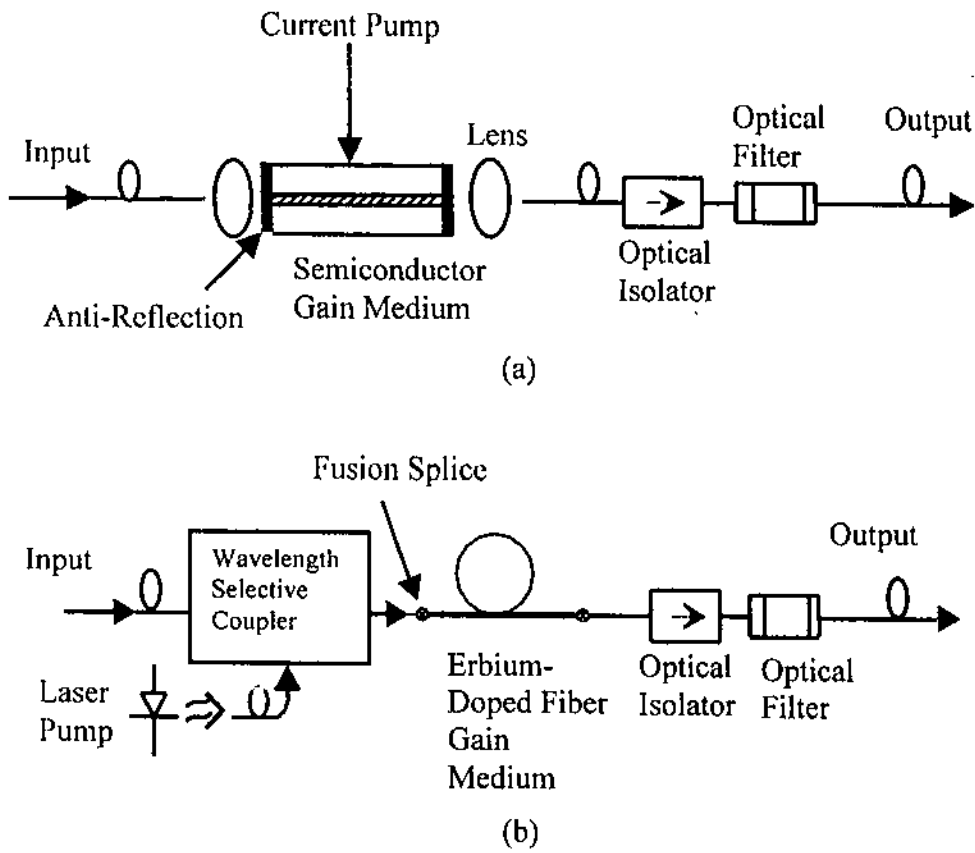
**Figure (1.4): Block diagram of (a) a semiconductor amplifier and (b) an erbium-doped fiber amplifier.**

## 1.4.3 Configuration and Construction of an EDFA

Figure (1.5) shows the three basic amplifier configurations corresponding to unidirectional; *forward* (or co-propagation), and *backward* (or counter-propagation) and bidirectional pumping. The main components of an EDFA are $Er^{3+}$-doped fiber, a light pump source, Wavelength selective couplers (WDM), and optical isolators. An optical filter may also be used.

- *WDM couplers:* The function of the WDM coupler in the module is to multiplex or demultiplex the signal and pump lights. The most significant properties of these wavelength-dependent couplers for signal and pump are the loss in both paths and the

splitting ratio or isolation (i.e. how completely the two channels are separated).
(Becker, et al.,1999).



(a)



(b)



( c )
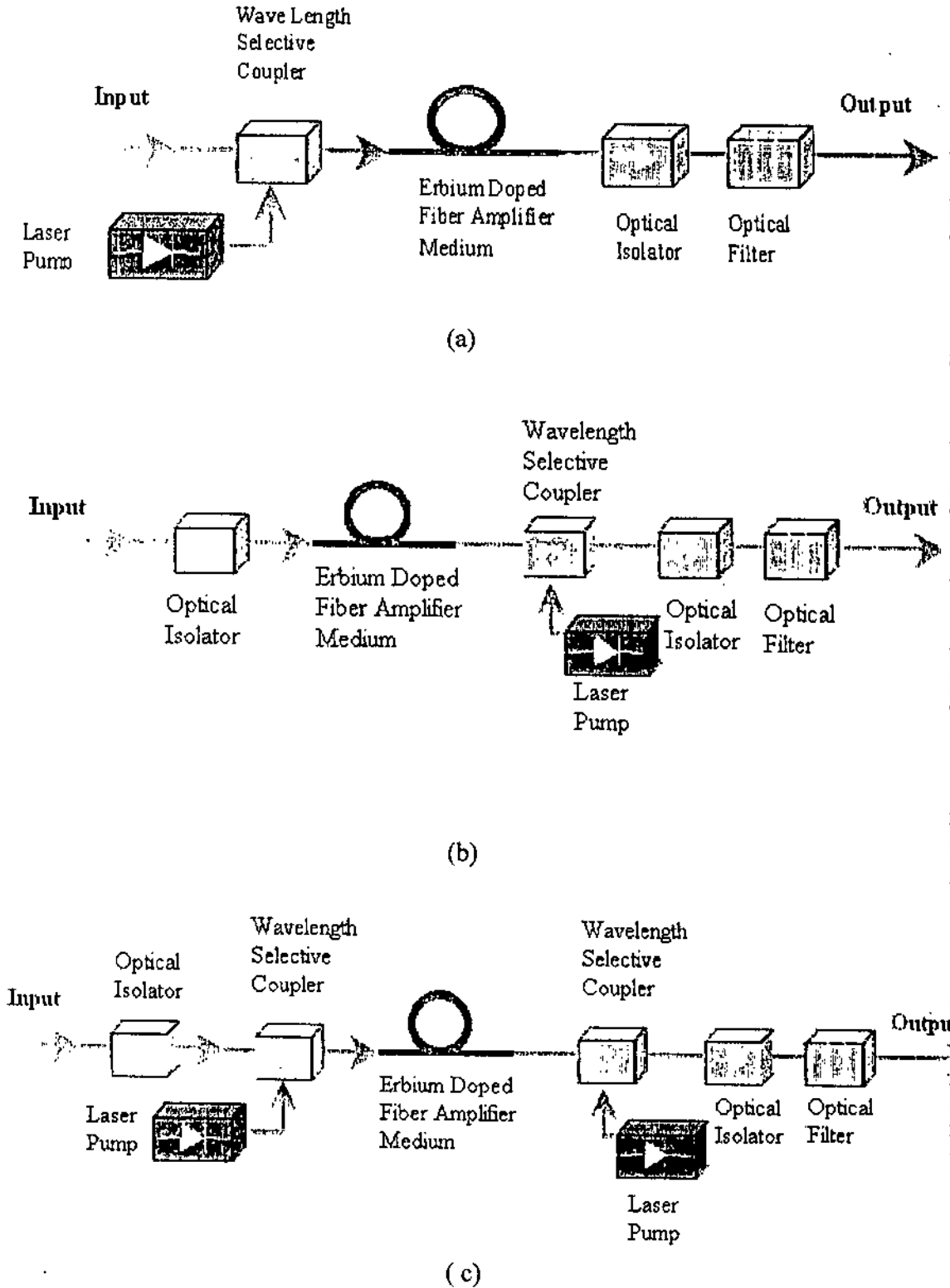
**Figure (1.5): Three basic amplifier configuration: (a) Forward pumping, (b) Backward pumping, (c) Bidirectional pumping**

- *Isolators :* Reflections at the input and output parts of an EDFA may have an effect on their performance. These reflections may cause the noise Figure, *NF*, of the EDFA to increase due to the inverted carriers amplifying an unwanted reflected field and not the desired signal. Reflections may also cause the EDFA to lase if the gain is high enough. Furthermore, an isolator may be necessary on the input side to prevent backward- travelling ASE from propagating back into reflection-sensitive components, such as a laser transmitter. (Becker, et al.,1999)

- *Filters:* Erbium-doped fiber amplifiers may use optical filters to enhance performance by suppressing amplified spontaneous emission either as it builds within the amplifier or at the end of a system span before detection. By inserting a bandpass filter of 1~2nm at the outside end of the EDFA the spontaneous shot and spontaneous-spontaneous beat noise (produced by the broadband ASE emanating from the amplifier) can be suppressed to achieve a reasonable SNR at the receiver. (Becker, et al.,1999).

- *Laser pumps:* The success of erbium-doped fiber amplifiers has been predicated on the commercial availability of reliable diode laser pumps with power sufficient to stimulate gain from the device. The most commonly used today are the 1480 nm and 980 nm diode lasers. They are typically packaged in a 14 pin butterfly package. The laser is usually sold with an integrated single mode fiber pigtail (Becker, et al.,1999).

- *The erbium-doped fiber*: The structure of erbium-doped fiber is almost the same as that of the conventional fiber used for optical transmission. However additional dopant materials, including $Er^{3+}$ are included in the core of the erbium-doped fiber. Also Erbium-doped fiber is of a smaller diameter than that of the conventional single mode fiber, (< 4μm) where it is (5~10)μm for a standard single mode fiber. A typical erbium-doped fiber is illustrated in Figure (1.6) shown below.
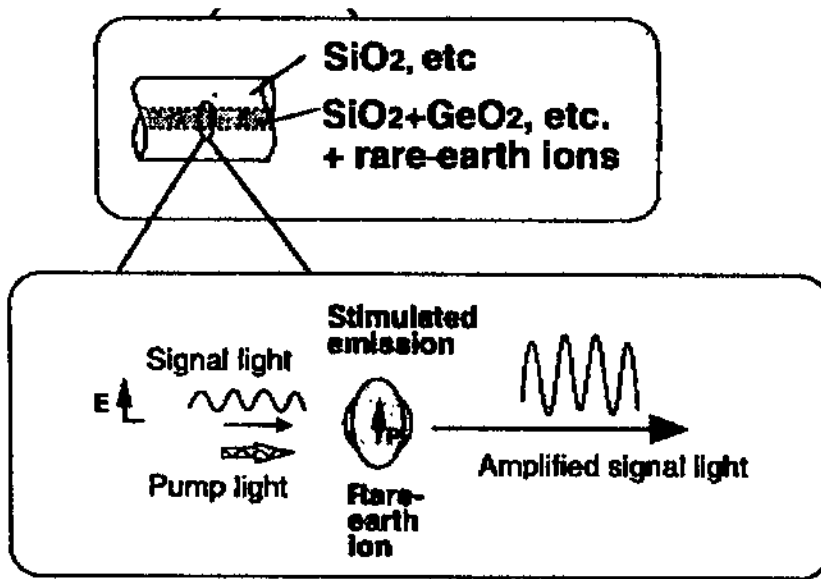


Figure 1.6: Basic structure and principle of optical signal amplification in EDFA

In order to achieve efficient amplification, requirements should be met. The first is that the erbium ions should operate in a radiative transition with high quantum efficiency. The second requirement is that efficient pumping should be realized. The third is that the fiber should exhibit low loss, including scattering loss and low absorption loss.

# 1.5 Properties of Erbium in Glass

To produce the amplifier gain medium, the silica fiber core of a standard single-mode fiber is doped with erbium ion. Because of many different energy levels in erbium, several wavelengths will be absorbed by the ion. Figure (1.7) shows the energy levels and some of the key wavelengths that can be absorbed.
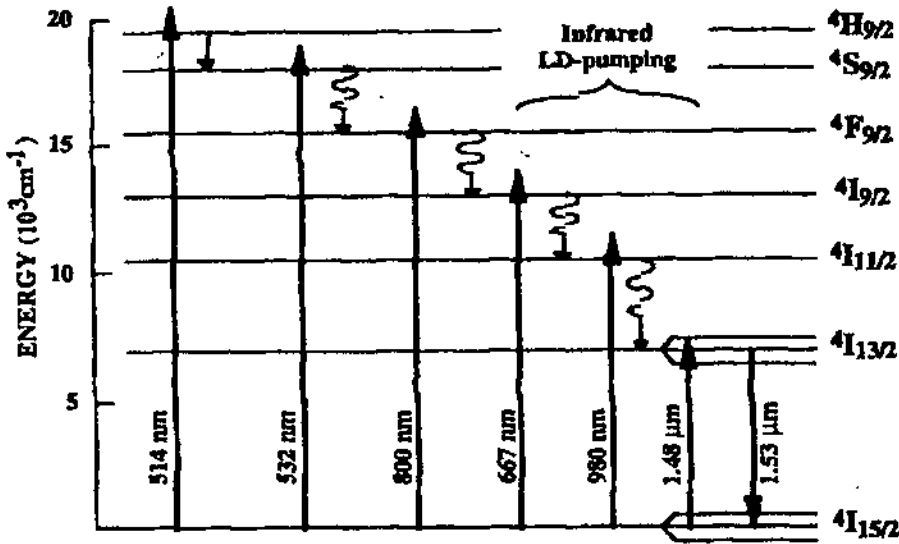


Figure (1.7): The energy levels of erbium

In general, absorption corresponds to a photon being absorbed and causing a carrier (ion) to jump to a higher energy level of energy difference, $\Delta E = h\nu$, that roughly matches the energy of the photon. Different wavelengths can cause either ground state absorption (GSA) or excited state absorption (ESA). GSA corresponds to a photon exciting a carrier from the ground state to a higher state, and ESA corresponds to a photon exciting a carrier from one of the non-ground state energy levels to an even higher level. Since the population is greatest in the ground state, the probability of GSA occurring is much greater than ESA. Once a photon is absorbed and a carrier is excited to a higher-energy level, the carrier decays rapidly to the first excited level. Once the

carrier is in the first excited state, it has a very long lifetime of ~10 ms, thereby enabling us to consider the first excited level to be metastable. Depending on the external optical excitation signal, this carrier will decay in a stimulated or spontaneous fashion to the ground state and emit a photon. The emission in erbium is fortunately near the 1.55 μm loss-minimum of standard silica optical fiber.

The absorption is not as strong for all the possible wavelengths, governed critically by the tendency of a pump photon to be absorbed as determined by the cross-section of the erbium ion with that photon. Figure (1.8) shows the absorption measured in an erbium-doped fiber at room temperature (Becker, et al.,1999). The erbium is doped in a core of germano-alumino-silica glass. The various peaks correspond to transitions between the $1^4_{15/2}$ ground state and the higher-lying states. The pump region at 1480 nm provides significant absorption.

Fortunately, high power multimode laser diodes for 1480 nm wavelength are commercially available, compact, reliable, and potentially inexpensive.
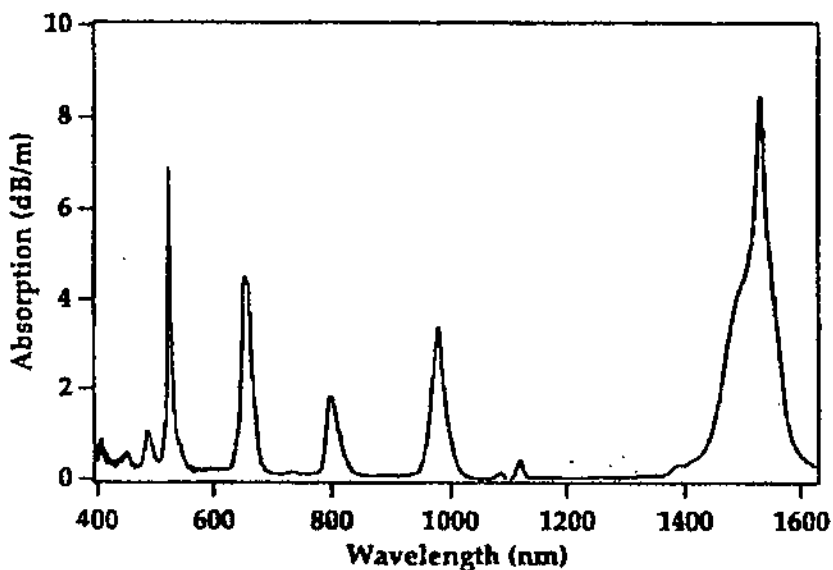


Figure (1.8) : Experimentally measured absorption spectrum of an $Er^{3+}$ doped germano-alumino-silica fiber [Becker,1999]

Both the absorption and emission spectra have an associated bandwidth. These bandwidths depend on the spread in wavelengths that can be absorbed or emitted from a given energy level, allowing multimode multiwavelength diode laser light to be absorbed. Such a spread in wavelengths is caused by Stark-splitting of the energy levels, allowing a deviation from an exact wavelength. This is highly desired because (1) the exact wavelength of the pump laser may not be controllable and is impossible for a multimode laser, and (2) the signal may be at one of several wavelengths, especially in a WDM system, that makes implementation of the amplifier very flexible. The spectrum of $Er^{3+}$ depends on the host glass. Figure (1.9) shows the absorption and emission spectra of $Er^{3+}$ near 1.5 $\mu$m representing the $I^4_{13/2} \leftrightarrow I^4_{15/2}$ transition, for Al-Ge-silica glass host (Becker, et al.,1999).
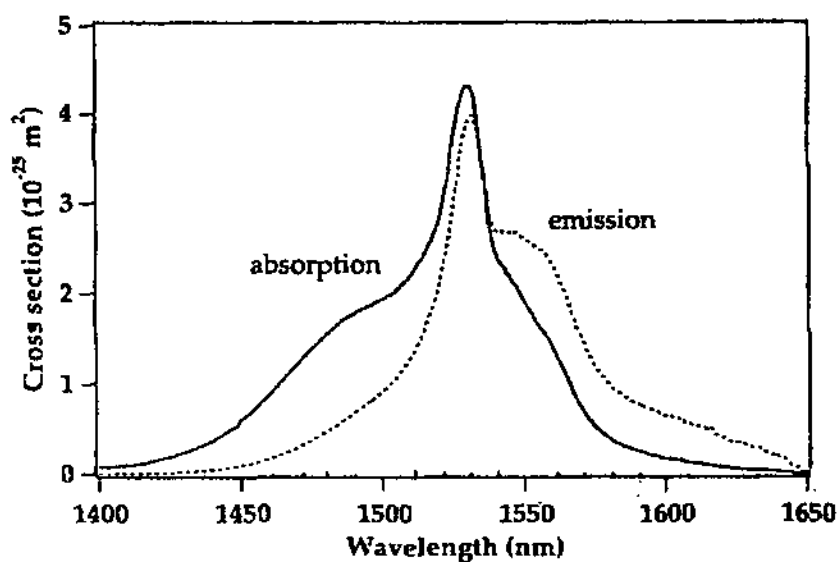


Figure (1.9): Absorption (solid line) and emission (dashed line) cross section of Er 3+ near 1.5 um, for an Al-Ge-Er-doped silica fiber (fiber A), [Becker,1999]

The erbium should be co-doped with another material in the fiber, for two reasons. First, erbium ions are quite large in comparison to silica atoms and are not very

soluble in silica, thereby making it difficult to highly dope the fiber so as to achieve high gain in a short length. Therefore another material that is more soluble in silica but similar in size to erbium is required to help incorporate more erbium in the fiber core region. A concentration of about one thousand parts per million can be attained by using co-dopants.

The second reason is that related to systems performance. Because we need multipurpose amplifier in different applications, the gain bandwidth should be as broad and as uniform as possible. The bandwidth of erbium doped fiber is only on the order of 10nm and exhibits a definite nonuniform structure. Incorporating co-dopant enhances the Stack-splitting of the various levels, thereby broadening and smoothing the gain profile.

# CHAPTER (2): MATHEMATICAL FRAMEWORK

## 2.1  Useful Background

The basis for the study of electromagnetic wave propagation is provided by Maxwell's equations (Senior,1992). For a medium with zero conductivity the vector relationships may be written in terms of the electric field $\mathbf{E}$ (V/m), magnetic field $\mathbf{H}$ (A/m), electric flux density $\mathbf{D}$ (C/m$^2$) and magnetic flux density $\mathbf{B}$ (W/m$^2$) as the curl equations:

$$\nabla x \mathbf{E} = \frac{-\partial \mathbf{B}}{\partial t} \tag{2.1}$$

$$\nabla x \mathbf{H} = \frac{\partial \mathbf{D}}{\partial t} \tag{2.2}$$

and the divergence conditions:

$$\nabla . \mathbf{D} = 0 \qquad \text{( no free charges)} \tag{2.3}$$

$$\nabla . \mathbf{B} = 0 \qquad \text{( no free poles)} \tag{2.4}$$

where $\nabla$ is a vector operator.

The four field vectors are related by the relations

$$\mathbf{D} = \varepsilon \mathbf{E} \tag{2.5}$$

$$\mathbf{B} = \mu \mathbf{H} \tag{2.6}$$

where $\varepsilon$ is the electric permittivity and $\mu$ is the permeability of the medium. The refractive index $n = \sqrt{\varepsilon_r}$ is usually used to specify the dielectric constant. The net permittivity of the medium, is written as the product, $\varepsilon = \varepsilon_r \varepsilon_0 = n^2 \varepsilon_0$.

## 2.1.1 Electromagnetic Wave Equations in Sourceless Media

Substituting for **D** and **B** and taking the curl of equation (2.1) and (2.2) will yield:

$$\nabla x \nabla x \mathbf{E} = -\mu \frac{d}{dt} \nabla x \mathbf{H} = -\mu \varepsilon \frac{d^2 \mathbf{E}}{dt^2} \tag{2.7}$$

Use the vector identity $\nabla x \nabla x \mathbf{E} = \nabla(\nabla.\mathbf{E}) - \nabla^2 \mathbf{E}$

Considering the core and the cladding as two separate mediums. Each one is considered to be homogeneous, meaning that $\varepsilon$ and $\mu$ do not vary with position. Therefore, Equation (2.7) becomes

$$\nabla^2 \mathbf{E} - \mu \varepsilon \frac{d^2 \mathbf{E}}{dt^2} = 0 \tag{2.8}$$

Following the same procedure with Equation (2.2), will yield to

$$\nabla^2 \mathbf{H} - \mu \varepsilon \frac{d^2 \mathbf{H}}{dt^2} = 0 \tag{2.9}$$

The solutions of equations (2.8) and (2.9) will be of the form of propagation functions which travels along the z-axis, take the following forms

$\mathbf{E} = E_0 \, g(t \pm (z/\underline{v}))$ and $\mathbf{H} = H_0 \, g(t \pm (z/v))$

where $v$ is the velocity of wave propagation and g is any function. Choosing the minus sign in the argument of g means that as t increases, an increase in z is necessary to maintain a fixed value of g. consequently, the function g (and hence the fields) will move in the positive z direction. Substituting the above forms of **E** or **H** into the appropriate wave equation and assuming variation with z and t only, leads to the wave velocity as $v = \dfrac{1}{\sqrt{\mu \varepsilon}}$ .

Let $\quad g(t) = e^{j(\omega t \pm /k - \phi)}$ $\tag{2.10}$

Where β the propagation constant defined as $\beta = \dfrac{\omega}{v}$, is the phase shift per unit distance of the sinusoidal wave measured along the z-axis. Since the function is sinusoidal, the wave velocity is known as the phase velocity $v$.

Furthermore, with t fixed, the function will go through one complete cycle in z when βz=2π.

The field in complex instantaneous form is expressed as:

$$E_c = E_o e^{j(\omega t \pm \beta z + \phi)} \tag{2.11}$$

Since ω is included in β, Equation (2.11) would adequately describe the wave if the time dependence $e^{j\omega t}$ were not included, which is equivalent to freezing the time at t=0. The resulting phasor form of the field becomes a useful simplified way of expressing a single wave or a combination of waves that are all at a single frequency, ω

$$E_c = E_o e^{\pm j\beta z + j\phi} \tag{2.12}$$

Returning back to Equation (2.8) and (2.9), and defining $k = \omega\sqrt{\mu\varepsilon}$, the wave equations will be

$$\nabla^2 \mathbf{E} + k^2 \mathbf{E} = 0 \tag{2.13}$$

$$\nabla^2 \mathbf{H} + k^2 \mathbf{H} = 0 \tag{2.14}$$

These two equations are known as the vector Helmholtz equations.

They form the staring point for the analysis of all types of waveguides that are constructed from linear, homogeneous, and isotropic materials.

As an example, consider a wave that propagates in the positive z-direction in a lossless material, suppose that the electric and magnetic fields lie in the plane transverse to the propagation direction (x-y), and furthermore, that they exhibit no variation in any

direction within the transverse plane. Such a wave is an example of a uniform plane wave. Under these conditions Equation (2.13) becomes:

$$\frac{d^2 E}{dz^2} + k^2 E = 0 \tag{2.15}$$

Whose solution is $E = E_0 e^{-jkz}$. Thus in the uniform plane wave. Case, $\beta = k = \omega\sqrt{\mu\varepsilon}$

The phasor from of the electric field can be written as

$$E = E(x, y, z) = E_o(x, y)e^{-j\beta z} \tag{2.16}$$

Equation (2.13) becomes

$$\nabla_t^2 E + (k^2 - \beta^2)E_o = 0 \tag{2.17}$$

Where the transverse Laplacian is $\nabla_t^2 = \frac{d^2}{dx^2} + \frac{d^2}{dy^2}$

It is seen that $\beta \neq k$ if the fields vary in the transverse direction to propagation. $\beta$ will thus depend on the transverse field variation which in turn is determined by the structure of the guide.

## 2.1.2 Optical Fibers with Single-Step Index Profiles

The single - step index fiber consists of two concentric homogeneous dielectrics, shown in Figure (2.1), the inner dielectric, or core, fills the region r<a and is of refractive index $n_1$. The outer material (r>a), known as the cladding, is of index $n_2$, where $n_2 < n_1$. The cladding is considered, for purposes of analysis, to be of infinite outer radius. Key structural parameters include the core radius, a, and the normalized index difference.

$$\Delta = \frac{n_1^2 - n_2^2}{2n_1^2} \cong \frac{n_1 - n_2}{n_1} = \frac{\delta_n}{n_1} \tag{2.17}$$

where $n_1$ is very close to $n_2$. Another important quantity is the numerical aperture, NA, defined as:

$$NA = \sqrt{n_1^2 - n_2^2} = n_1\sqrt{2\Delta} \tag{2.18}$$

Standards on dimensions have been set by various committees. Specifying a cladding diameter of 125 µm as the production standard for most single and multimode fibers. Core diameters vary between 50 and 100µm for multimode, and between 4 and 10 µm for single mode fibers. Values for $\Delta$ are typically about 0.2% for single mode, and about 1% for multimode.
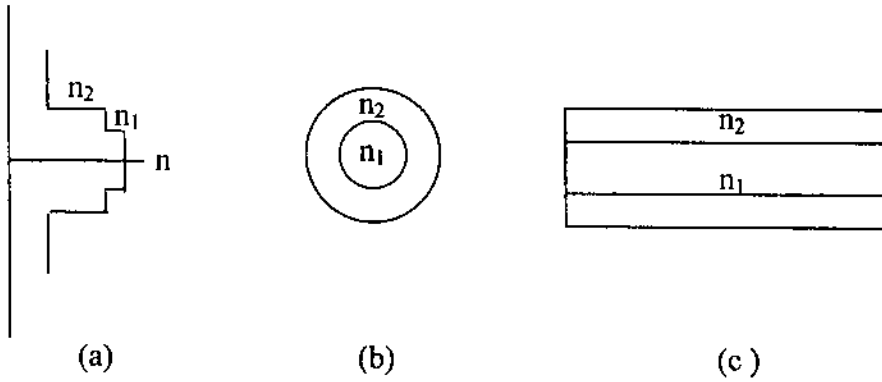


Figure 2.1: Step index fiber. (a) Refractive index profile. (b) End view. (c) Cross-sectional side view

## 2.1.3 Field Analysis of the Step Index Fiber

Field analysis begins by assuming field solutions of the form:

$\mathbf{E} = \mathbf{E}_o(r,\phi)e^{-j\beta z}$      and      $\mathbf{H} = \mathbf{H}_o(r, \phi)e^{-j\beta z}$

Using Equation (2.17)

$$\nabla_t^2 \mathbf{E}(r,\phi) + (k_1^2 - \beta^2)\,\mathbf{E}(r,\phi) = 0 \qquad r \le a \tag{2.19}$$

$$\nabla_t^2 \mathbf{E}(r,\phi) + (k_2^2 - \beta^2)\,\mathbf{E}(r,\phi) = 0 \qquad r \ge a \tag{2.20}$$

Where $k_1^2 - \beta^2 = \beta_{t1}^2$   and   $k_2^2 - \beta^2 = \beta_{t2}^2$

Assuming transverse variation in both r and $\phi$, the wave equation becomes in general,

$$\frac{\partial^2 E_z}{\partial r^2} + \frac{1}{r}\frac{\partial E_z}{\partial r} + \frac{1}{r^2}\frac{\partial^2 E_z}{\partial \phi^2} + \beta_t^2 E_z = 0 \tag{2.21}$$

It is assumed that the solution for $E_z$ will be a discrete series of modes, each of which has separated dependencies on r, $\phi$ and z in product form:

$$E_z = \sum_i R_i \ (r)\Phi_i(\phi)e^{-j\beta_i z} \tag{2.22}$$

Substituting one of the above modes into the wave equation (2.21) will yield:

$$\frac{r^2}{R}\frac{\partial^2 R}{\partial r^2} + \frac{r}{R}\frac{\partial R}{\partial r} + \beta^2 r^2 = -\frac{1}{\Phi}\frac{d^2\Phi}{d\phi} \tag{2.23}$$

The left-hand side of (2.23) depends only on r, whereas the right-hand side depends only on $\phi$, Since r and $\phi$ vary independently, it must follow that each side of Equation (2.23) must be equal to a constant. Defining this constant as $q^2$, Equation (2.23) separates into the following two equations:

$$\frac{d^2 R}{dr^2} + \frac{1}{r}\frac{dR}{dr} + (\beta_t^2 - \frac{q^2}{r^2})\,R = 0 \tag{2.24}$$

and

$$\frac{d^2\Phi}{d\phi^2} + q^2\Phi = 0 \tag{2.25}$$

Identifying the term $\frac{q}{r}$, it follows that $\beta_t^2 - \frac{q^2}{r^2} = \beta_r^2$. Solving (2.25) result in:

$$\Phi(\phi) = \begin{Bmatrix} \cos(q\phi + \alpha) \\ \sin(q\phi + \alpha) \end{Bmatrix} \tag{2.26}$$

q must be an integer, $\alpha$ is constant phase shift equation 24 will result in:

$$R(r) = \begin{Bmatrix} AJ_q(\beta_t r) & r \le a \\ CK_q(|\beta_t|r) & r \ge a \end{Bmatrix} \tag{2.27}$$

Where $J_q$ is ordinary Bessel function of the first kind, and of order q, which apply to cases of real $\beta_t$. If $\beta_t$ is imaginary then the solution will consist of modified Bessel functions, $K_q$. The solution in the core will be oscillatory, exhibiting no singularities and the solution in the cladding will monotonically decrease as radius increases.

The first solution suggests that the ordinary Bessel function should apply in the core region, and so $\beta_{t1} = \sqrt{k_1^2 - \beta^2}$ required to be real. The second condition indicates that $K_q$ function would exhibit the proper variation in the cladding. Therefore, $\beta_{t2} = \sqrt{k_2^2 - \beta^2}$ is required imaginary.

Defining the normalized propagation and attenuation constant as:

$$u = \beta_{t1}a = a\sqrt{k_1^2 - \beta^2} \tag{2.28}$$

$$w = |\beta_{t2}|a = a\sqrt{\beta^2 - k_2^2} \tag{2.29}$$

We find the complete solution for $E_z$ and $H_z$.

$$E_z = \begin{cases} AJ_q(\dfrac{ur}{a})\sin(q\phi)e^{-j\beta z} & r \le a \\ CK_q(\dfrac{wr}{a})\sin(q\phi)e^{-j\beta z} & r \ge a \end{cases} \tag{2.30}$$

and

$$H_z = \begin{cases} BJ_q(\dfrac{ur}{a})\sin(q\phi)e^{-j\beta z} & r \le a \\ DK_q(\dfrac{wr}{a})\sin(q\phi)e^{-j\beta z} & r \ge a \end{cases} \tag{2.31}$$

The transverse field components are found using Maxwell's equations. The resultant expressions are listed below:

$$r < a : \quad E_z = \left\{ AJ_q(\frac{ur}{a})\sin(q\phi) \right\} \tag{2.32}$$

$$E_r = \left\{ -A\frac{j\beta}{(u/a)}J_q{}'(\frac{ur}{a}) + B\frac{j\beta\mu}{(u/a)^2}\frac{q}{r}J_q(\frac{ur}{a}) \right\}\sin(q\phi)$$

$$E_\phi = \left\{ -A\frac{j\beta}{(u/a)^2}\frac{q}{r}J_q(\frac{ur}{a}) + B\frac{j\beta\mu}{(u/a)}J'_q(\frac{ur}{a}) \right\}\cos(q\phi)$$

$$r>a: \quad E_z = \left\{ CK_q(\frac{wr}{a})\sin(q\phi) \right\} \tag{2.33}$$

$$E_r = \left\{ C\frac{j\beta}{(w/a)}K_q{}'(\frac{wr}{a}) - D\frac{j\beta\mu}{(w/a)^2}\frac{q}{r}K_q(\frac{wr}{a}) \right\}\sin(q\phi)$$

$$E_\phi = \left\{ C\frac{j\beta}{(w/a)^2}\frac{q}{r}K_q(\frac{wr}{a}) + B\frac{j\beta\mu}{(w/a)}K'_q(\frac{wr}{a}) \right\}\cos(q\phi)$$

Similar equations is also derived for **H** components.

## 2.1.4 Mode Classification and the Eigenvalue Equation

With the transverse field components, eigenvalue equations can be derived to determine $\beta$, $u$, and $w$ for the modes. All field components that are tangent to the core-cladding boundary at r =a required to be continuous across it. Apply for all $\phi$ & z components will result in:

$$( \frac{J'_q(u)}{J_q(u)} + \frac{K'_q(w)}{wk_q(w)} )( \frac{n_1^2}{n_2^2}\frac{J_q(u)}{uj_q(u)} + \frac{K_q(w)}{wK_q(w)} ) = q^2 ( \frac{1}{u^2} + \frac{1}{w^2} )( \frac{n_1^2}{n_2^2}\frac{1}{u^2} + \frac{1}{w^2} ) \tag{2.34}$$

Using weakly guiding approximation which states that $n_1 \cong n_2$, equation (2.34) will be simplified to:

$$\frac{J'_q(u)}{uJ_q(u)} + \frac{K'_q(w)}{wK_q(w)} = \pm q( \frac{1}{u^2} + \frac{1}{w^2} )$$

1. q=0 which applies to TE and TM modes

$$\frac{J'_o(u)}{uJ_o(u)} = \frac{-K'_o(w)}{wK_o(w)}$$

Using $Z'_o = -Z_1$ for any cylindrical function

$$\frac{uJ_o(u)}{J_1(u)} = \frac{-wK_o(w)}{K_1(w)} \qquad TE_{om}, TM_{om} \tag{2.35}$$

2. For q>0, the right-hand side of (2.34) will be either positive or negative. With positive right hand side the eigenvalue equation for $EH_{qm}$ modes, with negative right-hand side, the equation for $HE_{qm}$ modes, using the following Bessel functions identities

$$Z_v^{'} = \frac{1}{2}(Z_{v-1} - Z_{v+1})$$

$$Z_{v+1}(X) + Z_{v-1}(X) = \frac{2v}{x}Z_v(X)$$

Equation (2.34) results in:

$$\frac{uJ_q(u)}{J_{q+1}(u)} = \frac{-wK_q(w)}{K_q(w)} \qquad EH_{qm}(q \geq 1) \qquad (2.36)$$

$$\frac{uJ_q(u)}{J_{q-1}(u)} = \frac{wK_q(w)}{K_{q-1}(w)} \qquad HE_{qm}(q \geq 1) \qquad (2.37)$$

Defining a new integer variable, $l$, Equations (2.35), (2.36) and (2.37) become:

$$u\frac{J_{l-1}(u)}{J_l(u)} = -w\frac{K_{l-1}(w)}{K_l(w)} \qquad (2.38)$$

where:

$$l = \begin{cases} 1 & TE_{0m}, TM_{0m} \\ q+1 & EH_{qm} \\ q-1 & HE_{qm} \end{cases}$$

Since it was proved that the electric field superposition of the combining modes is linearly polarized in the transverse plane; thus the composite modes are referred to as the $LP_{lm}$ modes.

## 2.1.5 Solution of the Eigenvalue Equations

A graphical solution is suggested here to solve for $TE_{0m}$, $TM_{0m}$ ($LP_{1m}$) and $HE_{1m}$ ($LP_{0m}$) modes. First define the normalized frequency parameter, V, as :

$$V = \sqrt{u^2 + w^2} = aK_o(n_1^2 - n_2^2)^{\frac{1}{2}} = n_1aK_o\sqrt{2\Delta} \tag{2.39}$$

This important parameter, often called the V number, embodies the fiber structural parameter and frequency. It is used together with equation (2.39) to find the propagation constants $u$, $w$, and $\beta$. Rewriting (2.35) to be read as:

$$\frac{J_1(u)}{J_0(u)} = \frac{-u}{w}\frac{K_1(w)}{K_0(w)} \tag{2.40}$$

and (2.37) becomes.

$$\frac{J_1(u)}{J_0(u)} = \frac{w}{u}\frac{K_1(w)}{K_0(w)} \tag{2.41}$$

The left-hand side of the two equations when plots as a function of u, will produce curves that resemble those of a tangent function. The right-hand side of (2.40) is plotted as a curve shown in the lower half-plane and that of (2.41) is plotted as a curve shown in the upper half-plane, as shown in Figure (2.2). Its intersection with $\frac{J_1}{J_0}$ curves indicates solution. The value of u thus obtained can be used to find w and $\beta$, knowing V.
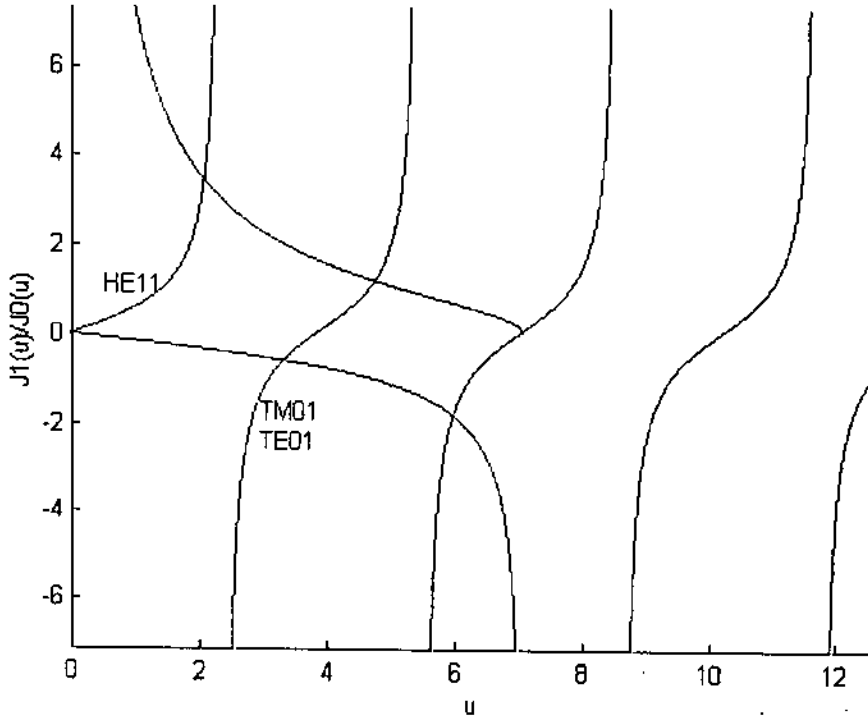
**Figure 2.2: Graphical solution for finding the propagation constant**

Getting $u$, from the graph, using equations (2.28) and (2.29), we get $w$, and $\beta$. And from equation (2.30) above, we get the transverse components as follows, taking into account to be understood with $e^{-j\beta z}$, with $E_0=j\beta Aa/u$ :

$HE_{qm}$:

$$E_r(r \le a) = -E_0 J_{q-1}(\frac{ur}{a})Sin(q\phi)$$

$$E_r(r \ge a) = -E_0 \frac{u}{w}\frac{J_q(u)}{K_q(w)}K_{q-1}(\frac{wr}{a})Sin(q\phi) \qquad (2.42)$$

$$E_\phi(r \le a) = -E_0 J_{q-1}(\frac{ur}{a})Cos(q\phi)$$

$$E_\phi(r \ge a) = -E_0 \frac{u}{w}\frac{J_q(u)}{K_q(w)}K_{q-1}(\frac{wr}{a})Cos(q\phi) \qquad (2.43)$$

## 2.1.6 LP Modes

Actually, in an ideal fiber, the light will maintain its linear polarization, and so degenerate modes must superimpose in such a way to accomplish this. For the $LP_{0m}$ case, only the $HE_{1m}$ mode is present. Using the coordinate transformation;

$$E_x = E_r \cos\phi - E_\phi \sin\phi \quad \text{and} \quad E_y = E_r \sin\phi - E_\phi \cos\phi$$

The resulting Cartesian fields (either $E_x$ or $E_y$) for the single mode will be:

$$\mathbf{E}_{LP01} = E_0 J_0\left(\frac{ur}{a}\right) \qquad\qquad r \leq a \qquad\qquad (2.44)$$

$$\mathbf{E}_{LP01} = E_0 \frac{J_0(u)}{K_0(w)} K_0\left(\frac{wr}{a}\right) \qquad\qquad r \geq a \qquad\qquad (2.45)$$

Experimentally, the LP modes are observed as intensity patterns, proportional to $EE^*$ By using (2.44) and (2.45), the intensity function in the core and cladding for single mode fiber of 1.4μm core radius is shown in Figure (2.3) below, as achieved from a computer program.
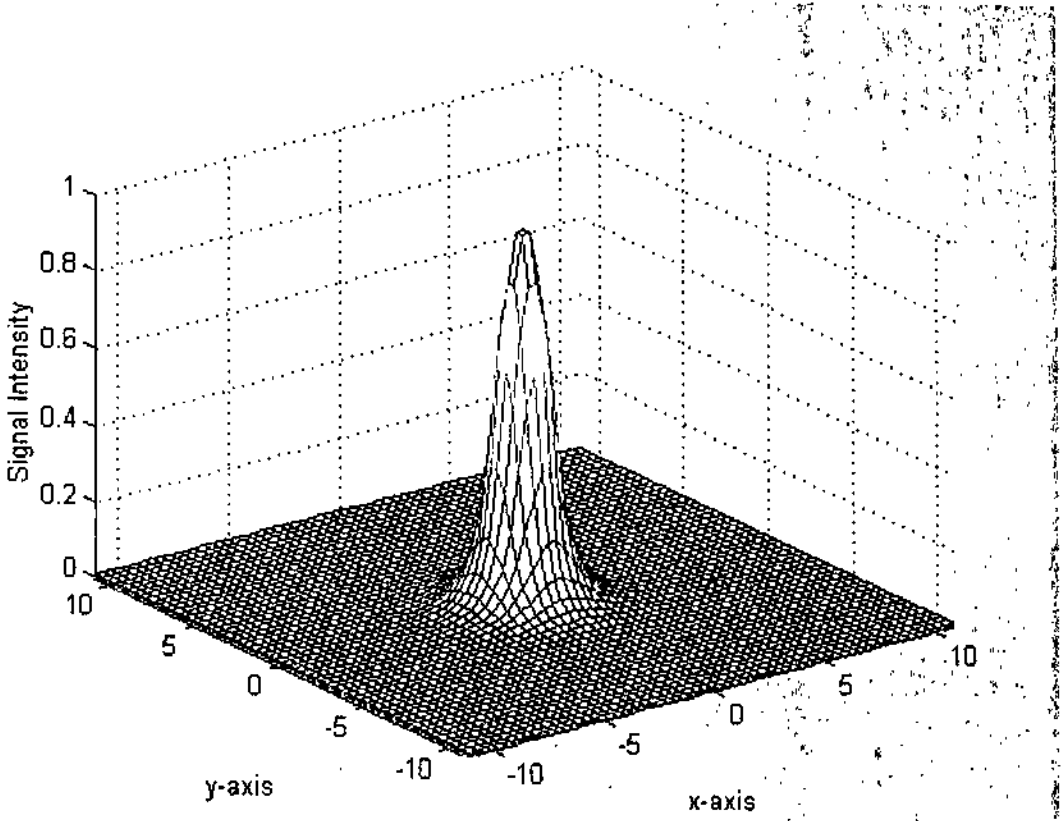
**Figure 2.3: Signal intensity profile**

## 2.2 Propagation and Rate Equations

### 2.2.1 Three-Level Rate Equations

As discussed previously in section 1.4, specially by investigating Figure (1.7). The most simple treatment of EDFA starts out by considering a pure three-level atomic system. (Desurvire,1994). Let us consider a three-level system as depicted in Figure (2.4), by definition, level 1 is the ground level, level 2 is the metastable level characterized by a long lifetime $\tau$, and level 3 is the pump level. The laser transition of interest takes place between levels 1 and 2.
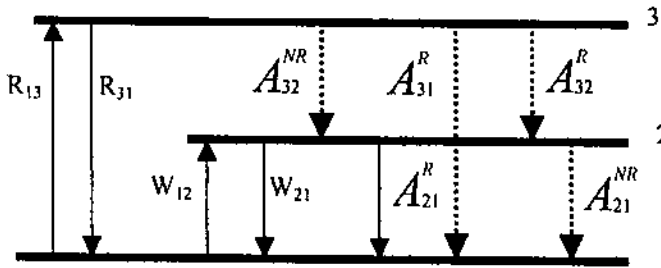


Figure 2.4: Energy level diagram corresponding to a basic three-level laser system

The pumping rate from levels 1 and 3 is $R_{13}$ and the stimulated emission rate between levels 3 and 1 is $R_{31}$. From the excited state corresponding to level 3, there are two possibilities of decay, i.e. radiative (rate $A_3^R = A_{32}^R + A_{31}^R$ ) and nonradiative (rate $A_{32}^{NA}$ ). The spontaneous decay from level 3 is assumed to be predominantly nonradiative, i.e., $A_{32}^{NA} >> A_3^R$. The stimulated absorption and emission rates between levels 1 and 2 are $W_{12}$ and $W_{21}$, respectively. The spontaneous radiative and nonradiative decay from the excited state corresponding to level 2 is $A_2 = A_{21}^R + A_{21}^{NR}$, with $A_{21}^R = 1/\tau$, where by definition $\tau$ is the fluorescence lifetime. It is assumed that the spontaneous decay is essentially radiative, i.e., $A_{21}^R >> A_{21}^{NR}$. In the following, the spontaneous decays from levels 2 and 3 will be more simply referred to as $A_{21}$ and $A_{32}$.

Let $\rho$ be the laser ion density and $N_1$, $N_2$, and $N_3$ the fractional densities, or populations, of atoms in the energy states 1, 2, and 3, respectively. By definition, $N_1 + N_2 + N_3 = \rho$. We can now write the atomic rate equations corresponding to these populations

$$\frac{dN_1}{dt} = -R_{13}N_1 + R_{31}N_3 - W_{12}N_1 + W_{21}N_2 + A_{21}N_2 \tag{2.46}$$

$$\frac{dN_2}{dt} = W_{12}N_1 - W_{21}N_2 - A_{21}N_2 + A_{32}N_3 \tag{2.47}$$

$$\frac{dN_3}{dt} = R_{13}N_1 - R_{31}N_3 - A_{32}N_3 \tag{2.48}$$

We consider now the steady state regime where the population are time invariant, i.e.,

$$\frac{dN_1}{dt} = \frac{dN_2}{dt} = \frac{dN_3}{dt} = 0 \tag{2.49}$$

We obtain from Equations (2.46)-(2.49):

$$W_{12}N_1 - (W_{21} + A_{21})N_2 + A_{32}N_3 = 0 \tag{2.50}$$

$$R_{13}N_1 - (R_{31} + A_{32})N_3 = 0 \tag{2.51}$$

Replacing $N_3$ by $\rho - N_1 - N_2$ in the above and solving for $N_1$, $N_2$ yields:

$$N_1 = \rho \frac{(R_{31} + A_{32})(W_{21} + A_{21})}{(W_{21} + A_{21})(R_{31} + A_{32} + R_{13}) + (R_{31} + A_{32})W_{12} + R_{13}A_{32}} \tag{2.52}$$

$$N_2 = \rho \frac{R_{13}A_{32} + (R_{31} + A_{32})W_{21}}{(W_{21} + A_{21})(R_{31} + A_{32} + R_{13}) + (R_{31} + A_{32})W_{12} + R_{13}A_{32}} \tag{2.53}$$

By factorization the term $A_{21}A_{32}$ in the above Equations, we obtain:

$$N_1 = \rho \frac{(1 + W_{21}\tau)(1 + \frac{R_{13}}{A_{32}})}{(1 + W_{21}\tau)(1 + \frac{R_{13} + R_{31}}{A_{32}}) + W_{12}\tau(1 + \frac{R_{31}}{A_{32}} + R_{13}\tau)} \tag{2.54}$$

$$N_2 = \rho \frac{R_{13}\tau + W_{21}\tau(1 + \frac{R_{13}}{A_{32}})}{(1 + W_{21}\tau)(1 + \frac{R_{13} + R_{31}}{A_{32}}) + W_{12}\tau(1 + \frac{R_{31}}{A_{32}} + R_{13}\tau)} \tag{2.55}$$

Assuming now that the nonradiative decay rate $A_{32}$ dominates over the pumping rates $R_{13,31}$, i.e., $A_{32} \gg R_{13,31}$, and Equations (2.54) and (2.55) yield:

$$N_1 = \rho \frac{(1 + W_{21}\tau)}{1 + W_{21}\tau + W_{12}\tau + R_{13}\tau} \qquad (2.56)$$

$$N_2 = \rho \frac{R_{13}\tau + W_{21}\tau}{1 + W_{21}\tau + W_{12}\tau + R_{13}\tau} \qquad (2.57)$$

With the above result, we find that $N_3 = \rho - N_1 - N_2 = 0$, i.e., the pump level population is negligible due to the predominant nonradiative decay ($A_{32}$) toward the metastable level 2. This applies specially when pumping at 980nm. Now let us pump at 1480nm, the $Er^{3+}$ -ion is excited from the ground state level, $I^4_{15/2}$, to the second level, $I^4_{13/2}$, this means that the EDFA acts as two-level laser system. This quasi-two-level system, shown in Figure (2.5), can be used to model optical amplification.

## 2.2.2 Quasi-Two-Level Rate Equations

The pump(signal) absorption and emission rates are $R_{12}(W_{12})$ and $R_{21}(W_{21})$, respectively. Spontaneous transitions from the excited state to the ground state are taken into account by the rate $A_{21}=1/\tau$; $\tau$ is the fluorescence life time. The absorption and emission rate of the amplified spontaneous emission are $W^{ASE}_{12}$ and $W^{ASE}_{21}$, respectively.
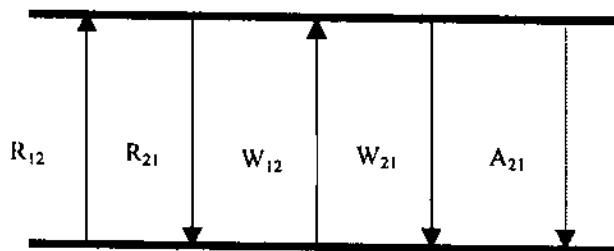


Figure 2.5 : Quasi Two-Level model for erbium energy

In order to analyze the intersection of the pump / signal photons with rate equations that can be deduced from the excitation scheme shown in Figure (2.5) as follows:

$$\frac{dN_1}{dt} = -(R_{12} + W_{12})N_1 + (A_{21} + R_{21} + W_{21})N_2 \tag{2.58.a}$$

$$\frac{dN_2}{dt} = -\frac{dN_1}{dt} \tag{2.58.b}$$

The EDFA is described in a $(r,\varphi,z)$- cylindrical coordinate system with the z-axis as fiber axis. Considering only $LP_{01}$-modes and a circular symmetry for the EDFA. $N_1(r,z)$ and $N_2(r,z)$ are the population concentration in the grounded and excited state respectively. The total Er- dopant concentration is $N_0(r)$ (no - z- dependence) such that

$$N_0(r) = N_1(r,z) + N_2(r,z) \tag{2.59}$$

Under steady-state conditions, all time derivatives in Equations (2.58) are zero. The resulting steady state rate equations will be;

$$N_1(r,z) = N_{0(r)} \frac{R_{21}(r,z) + W_{21}(r,z) + A_{21}}{(R_{21}(r,z) + R_{12}(r,z)) + (W_{21}(r,z) + W_{12}(r,z)) + A_{21}}$$

$$N_2(r,z) = N_0(r) - N_1(r,z) \tag{2.60}$$

The transition rates are determined as follows. The pump absorption rate:

$$R_{12}(r,z) = \sigma_{12} \cdot \frac{P_p(z)}{h\nu_p} I_p^{01}(r) \tag{2.61}$$

(Pedersen, et al.,1991). Where $\sigma_{12}$ is the absorption cross section at the pump wavelength, $P_p(z)$ is the pump power at position z in the fiber, h is Plank's constant, $\nu_p$ is the pump frequency, and $I_p^{01}(r)$ is the normalized $LP_{01}$ - mode, derived previously in this chapter, such that $2\pi \int_0^\infty I_p^{01}(r)r dr = 1$, at the pump wavelength. Here $I_p^{01}(r,\varphi,z)$ is assumed to be separable such that its shape is independent on $z$. The pump emission rate is:

$$R_{21}(r,z) = \sigma_{21} \cdot \frac{P_p(z)}{h v_p} I_p^{01}(r) \tag{2.62}$$

Where $\sigma_{21}$ is the emission cross section at 1.48 μm.

The signal emission and absorption rates, $W_{21}$ and $W_{12}$, are given by:

$$W_{21}(r,z) = \sigma_{21} \cdot \frac{P_s(z)}{h v_s} I_s^{01}(r) \tag{2.63}$$

$$W_{12}(r,z) = \sigma_{12} \cdot \frac{P_s(z)}{h v_s} I_s^{01}(r) \tag{2.64}$$

where $\sigma_{21}$ and $\sigma_{12}$ are the emission and absorption cross sections, respectively at the frequency $v_s$, $v_s$ is the signal frequency.

The equations that describe the propagation through the fiber are given by:

$$\frac{dP_s(z)}{dz} = \left[ \gamma_e(v_{s,z}) - \gamma_a(v_s, z) \right] P_s(z) \tag{2.65}$$

$$\frac{dP_p(z)}{dz} = u_p \left[ \gamma_e(v_{p,z}) - \gamma_a(v_p, z) \right] P_p(z) \tag{2.66}$$

Where the emission, $\gamma_e(v,z)$, and absorption, $\gamma_e(v,z)$, factors are determined from emission and absorption cross sections, respectively, and the overlap integral between the signal (pump) mode and the population concentration in the excited and ground state, respectively.

$$\gamma_e(v_k, z) = \sigma_{21}(v_k).2\pi \int_0^{a_d} N_2(r,z) I_k^{01}(r) r \, dr \tag{2.67.a}$$

$$\gamma_a(v_k, z) = \sigma_{12}(v_k).2\pi \int_0^{a_d} N_1(r,z) I_k^{01}(r) r \, dr \tag{2.67.b}$$

where k, is either s for signal, or p for pump, $a_d$ is the erbium doping radius. Finally $(u_p=1)$ for forward propagation and $(u_p=-1)$ for backward direction of the fiber.

Taking into consideration possible background loss $\alpha_k$, in the propagation along the fiber, Equations (2.65) and (2.66) would be:

$$\frac{dP_s(z)}{dz} = \left[\gamma_e(v_s,z) - \gamma_a(v_s,z)\right]P_s(z) - \alpha_s P_s(z) \qquad (2.65)'$$

$$\frac{dP_p(z)}{dz} = u_p\left[\gamma_e(v_p,z) - \gamma_a(v_p,z)\right]P_p(z) - \alpha_p P_p(z) \qquad (2.66)'$$

Throughout this work, background losses are defined to include the total losses associated by the amplifying fiber. These losses are classified into intrinsic and extrinsic factors; where intrinsic losses describe the attenuation mechanism associated by the physical properties of host materials. Extrinsic losses are originated from impurities (e.g. rare-earth ions except doped ions), (Sudo, 1997).

These equations are the general equations used in the recent work for modeling. They need to be solved numerically which will be discussed in details in the next chapter.

# CHAPTER (3): AMPLIFIER SIMULATION

## 3.1 Introduction

In this chapter the most important aspects involved in modeling the gain and basic behavior of EDFA will be discussed. The basic tools for modeling were developed using the modeling equations in the previous chapter. This modeling allows us to follow the signal and pump fields as they propagate along the fiber, and determine the population inversion. It leads to better understanding of the amplifications process, and gives some useful signs for designing an amplifier for different applications.

A well-known fiber, fiber A, (Becker, et al.,1999) which is Al-Ge-Er-doped silica fiber, is used in the simulation. Fiber A has a core radius of 1.4 µm, a Δn of 0.026 (refractive index difference between core and cladding), a numerical aperture of 0.28, The fiber has an $Er^{3+}$ concentration of $N_0=0.7 \times 10^{25}$ $m^{-3}$, with radius of distribution = 1.4 µm (assumed flat-top unless otherwise specified).

## 3.2 Model Realization

In the previous chapter we reached to the equations that determine the signal and pump power evolution; which is given in Equation (3.1) and (3.2).

$$\frac{dP_s(z)}{dz} = [\gamma_e(v_s,z) - \gamma_a(v_s,z)] P_s(z) - \alpha_s P_s(z) \tag{3.1}$$

$$\frac{dP_p(z)}{dz} = u_p [\gamma_e(v_p,z) - \gamma_a(v_p,z)] P_p(z) - \alpha_p P_p(z) \tag{3.2}$$

Where the emission and absorption factors are defined as

$$\gamma_e(v_s,z) = \sigma_{21}(v_s).2\pi \int_0^{a_d} N_2(r,z) I_s^{01}(r) r \, dr \tag{3.1.a}$$

$$\gamma_a(v_s, z) = \sigma_{12}(v_s).2\pi \int_0^{a_d} N_1(r,z) I_s^{01}(r) r dr \qquad (3.1.b)$$

$$\gamma_e(v_p, z) = \sigma_{21}(v_p).2\pi \int_0^{a_d} N_2(r,z) I_p^{01}(r) r dr \qquad (3.2.a)$$

$$\gamma_a(v_p, z) = \sigma_{12}(v_p).2\pi \int_0^{a_d} N_1(r,z) I_p^{01}(r) r dr \qquad (3.2.b)$$

The other parameters are defined from rate equations

$$N_1(r,z) = N_{0(r)} \frac{R_{21}(r,z) + W_{21}(r,z) + A_{21}}{(R_{21}(r,z) + R_{12}(r,z)) + (W_{21}(r,z) + W_{12}(r,z)) + A_{21}} \qquad (3.3.a)$$

$$N_2(r,z) = N_0(r) - N_1(r,z) \qquad (3.3.b)$$

$$R_{12}(r,z) = \sigma_{12}.\frac{P_p(z)}{hv_p} I_p^{01}(r) \qquad (3.3.c)$$

$$R_{21}(r,z) = \sigma_{21}.\frac{P_p(z)}{hv_p} I_p^{01}(r) \qquad (3.3.d)$$

$$W_{21}(r,z) = \sigma_{21}.\frac{P_s(z)}{hv_s} I_s^{01}(r) \qquad (3.3.e)$$

$$W_{12}(r,z) = \sigma_{12}.\frac{P_s(z)}{hv_s} I_s^{01}(r) \qquad (3.3.f)$$

$I_s^{01}(r)$ and $I_p^{01}(r)$ are the normalized intensity for both signal and pump respectively

such that,

$$2\pi \int_0^\infty I_s^{01}(r) r dr = 1 \qquad (3.3.g)$$

$$2\pi \int_0^\infty I_p^{01}(r) r dr = 1 \qquad (3.3.h)$$

Here $I_k(r,\varphi,z)$ is assumed to be separable such that the shape of the $k^{th}$ optical mode is

independent of z.

$\alpha_p$ and $\alpha_s$ are the background losses due to pump wavelength and signal wavelength respectively.

In this work, Equations (3.1) and (3.2) are solved numerically, since $N_1$ and $N_2$, and thus the overlap integration are z-dependant variables. In the numerical scheme used here, the fiber length is divided into small sections ($\Delta z$) such the overlap integrals can be considered constant, such that the differential equations are approximately by difference ones. This method is illustrated graphically in Figure (3.1) below:
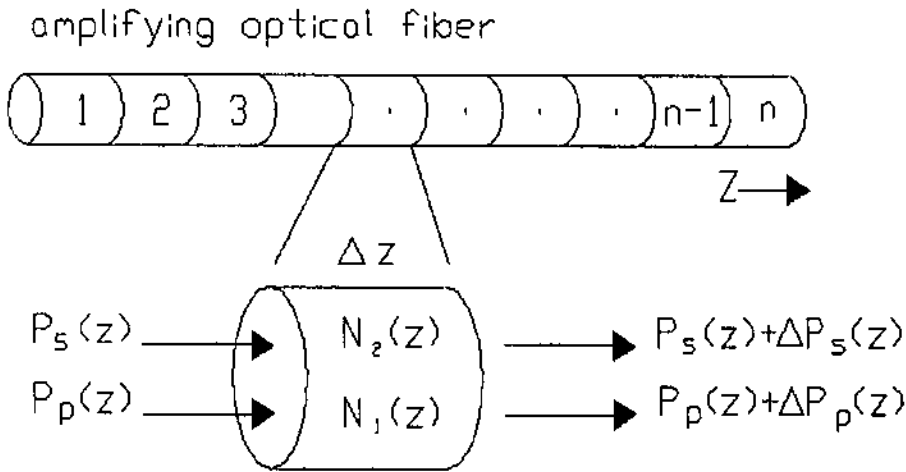
Figure 3.1: Fiber sectioning

So equation (3.1) and (3.2) will be respectively:

$$dP_s = \alpha_s' \, P_s \, dz \qquad (3.4.a)$$

$$dP_p = \alpha_p' \, P_p \, dz \qquad (3.4.b)$$

Where $\alpha_s'$, and $\alpha_p'$ is called gain factor and defined as $\gamma_e(v_s,z)-\gamma_a(v_s,z)-\alpha_s$ and $\gamma_e(v_p,z)-\gamma_a(v_p,z)-\alpha_p$ respectively.

Equation (3.4.a) and (3.4.b) can then be solved analytically as:

$$P_s(\Delta z) = P_0 \, e^{\alpha_s' \, \Delta z} \qquad (3.5.a)$$

$$P_p(\Delta z) = P_0 \, e^{\alpha_p' \, \Delta z} \qquad (3.5.b)$$

Or in general:

$$P_N = P_{N-1} e^{\alpha \Delta z}$$

(3.6)

Equation (3.5) and (3.6) are applied for both Equations (3.1) and (3.2).

.    . The milestone here is to identify all the parameters needed to find $\alpha$ at each step. Those parameters are classified in the following categories:

1.  System requirements: which includes signal wavelength and initial signal power $S_0$.

2.  Erbium characteristics: which include erbium spectrum (florescence) curves and life time ($\tau$) tables. These characteristics also depend on dopant materials (hosts) as for example shown in Figure (3.2) below

From these Figures, the absorption and emission cross sections can be obtained for different wavelengths. An example of such cross sections is listed below in table (3.1) (Becker, et al.,1999).

Table 3.1: Absorption ($\sigma_{abs}$) and emission ($\sigma_{em}$) cross sections in $Er^{+3}$ at the indicated wavelengths units of $10^{-21}$ cm$^2$ for various glass hosts

| Host Glass | Wavelength (nm) | $\sigma_{abs}$ ($\times 10^{-21}$ cm$^2$) | $\sigma_{em}$ ($\times 10^{-21}$ cm$^2$) |
|---|---|---|---|
| $GeO_2$-$SiO_2$ | 1530 | $7.9 \pm 0.3$ | $6.7 \pm 0.3$ |
| $Al_2O_3$-$SiO_2$ | 1530 | $5.1 \pm 0.6$ | $4.4 \pm 0.6$ |
| $GeO_2$-$Al_2O_3$-$SiO_2$ | 1530 | $4.7 \pm 1.0$ | $4.4 \pm 1.0$ |
| $GeO_2$-$Al_2O_3$-$SiO_2$ | 1480 | 1.5 | 0.5 |
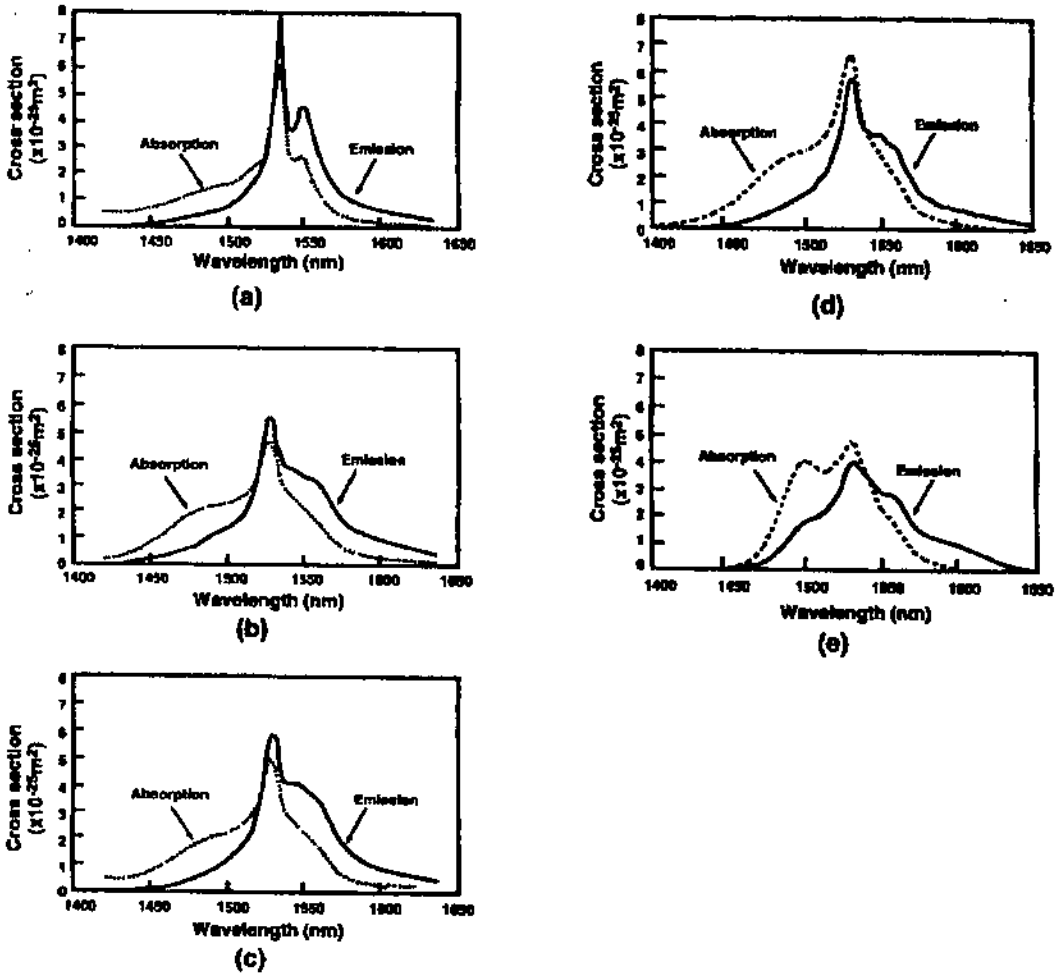
**Figure 3.2: Typical absorption and emission cross-section spectra (a) Ge/Er-doped silica glass (b) Al/Er-doped silica glass (c) Ge/Al/Er-doped silica glass (d) Al/P/Er-doped silica glass (e) ZrF4 based fluoride glass**

Also from previous works, lifetime τ can also be obtained, as shown in table (3.2) below (Becker, et al.,1999).

**Table 3.2: Lifetime (ms) for Er$^{+3}$ for various glass hosts**

| Host Glass | Lifetime (ms) |
|------------|---------------|
| Al-Ge silica | 9.5-10.0 |
| Silicate | 14.7 |
| Al-P silica | 10.8 |

3. EDFA structure: which is classified by:

- Initial pump power $P_0$, and pump wavelength $\lambda_p$ which is taken to be 1480nm to ensure two-level energy system.

- Core radius: which as specified early in this work to be < 4 µm (Kazovsky, et al.,1996) for single mode.

- Refractive index profile: taken here to be step-like, with very small core radius to ensure dispersion shift configuration.

- $Er^{3+}$ concentration profile: Two profiles here are investigated; the Gaussian shape profile, and the step-like profile. The first profile was chosen to approximately follow the pump intensity profile, while the second to follow the index profile. Usually the concentration is given by ions/volume unit. .

Two separate subroutines were built to prepare the data files that contain the index profile and the $Er^{3+}$ concentration profile respectively. Each point in the linear matrix shown in Figure (3.3) will have its own value.
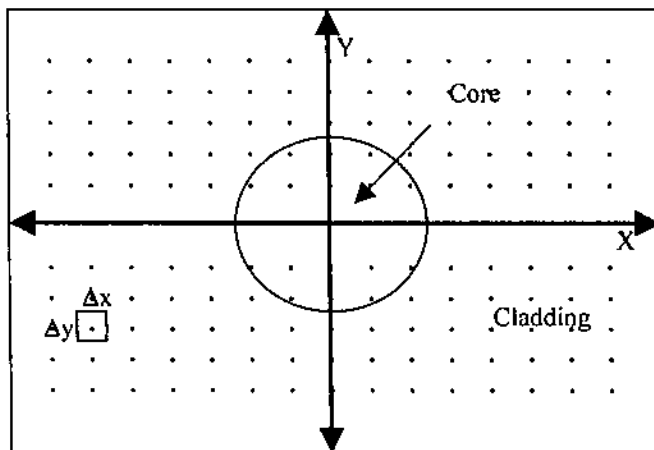


Figure 3.3: Computational grid showing the core and enough portion of the cladding
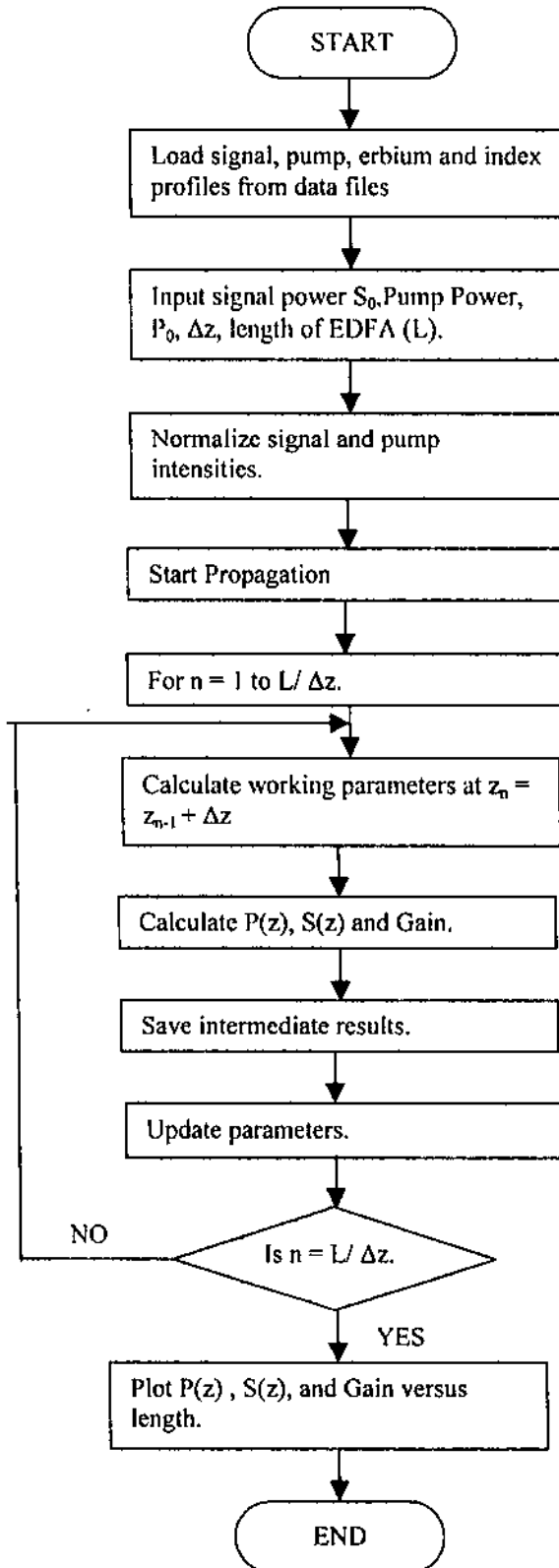
## 3.3   Flow charts



**Figure3.4: Flow chart showing the main block program used to simulate the signal gain as it propagates along the fiber**

# 3.4 Design Issues

The gain obtained from the amplifier is the most important measure of the EDFA performance. Throughout this chapter, the gain will be discussed by interplay of several EDFA parameters:

1) The pump launched power, $P_0$

2) The EDFA fiber length L.

3) The erbium concentration profile and value $N_0$.

4) Pump propagation direction (forward or backward).

5) Fiber Numerical Aperture (NA).

## 3.4.1 Signal Gain Versus Pump Power

First a specific fiber length will be considered, the mechanics of gain process for that length will be investigated. We start by considering a 14m length of fiber A. The signal and pump are taken to be copropagating and injected at z=0. The gains at two signal wavelengths of 1530 nm and 1550 nm are computed as a function of pump power, Figure (3.5). These two signal wavelengths are chosen because they are representative of the two main regions of the EDFA, the strong narrow peak near 1530 nm, and the flatter plateau around 1550 nm. They are quite different in terms of the ratio emission to absorption cross section. The injected signal power is taken to be a small signal value (0.1 μW). The pump wavelength considered is 1480nm, the background losses $\alpha_s$ and $\alpha_p$ are taken to be 0.03 dB/m (Giles and Desurvire,1991).
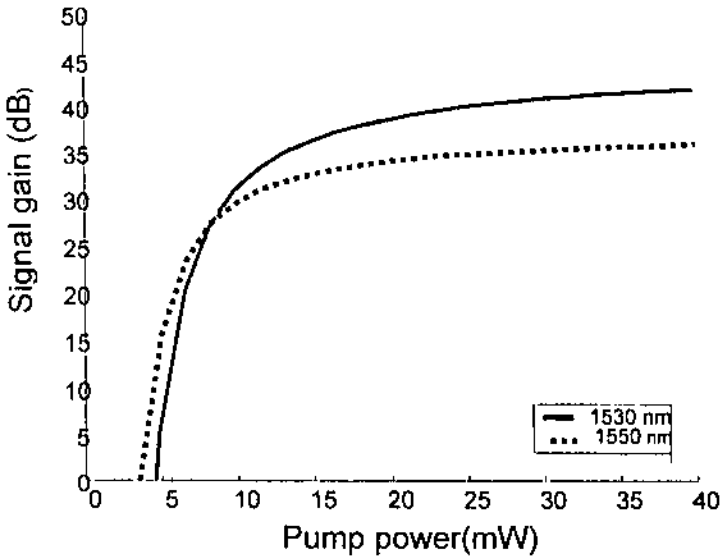
**Figure 3.5: Gain as a function of pump power for 14 m length of erbium-doped Al-Ge-silica fiber (fiber A) pumped at 1480 nm. $\lambda_s$ _ 1530nm (Solid curves), and $\lambda_s$ _ 1550nm (dotted curves).**

It does worth to mention here several points about Figure (3.5) above:

- For high pump powers, the gain for 1530 nm is higher than that for 1550 nm, due to its higher emission cross section compared to that at 1550 nm, since when the fiber is well inverted ($N_2 \approx N_0$) the gain is simply proportional to the emission cross section.

- At low pump powers, the gain factor becomes strongly dependant on the ratio between the emission and absorption cross sections as well as to the exact distribution of the population between the upper and lower states. The absorption at 1550 nm is significantly lower than that at 1530 nm, so that a smaller amount of pump power is needed to reach threshold (pump power required for fiber transparency (Gain = 0 dB)) for a 1550 nm signal than that for 1530nm one.

The next step is to investigate what will happen if the length of the fiber is changed for certain signal wavelength. Consider for example Figure (3.6), in which the gain is computed as a function of pump power for fiber lengths of 5, 10, 15, and 20 m

of fiber A. The signal of wavelength 1550 nm and the pump wavelength 1480 nm are taken to be copropagating and injected at $z=0$. As can be noted the gain strongly depends upon the EDFA length, it increases by length's increase. Also it is noticeable that as the length is increased, the threshold pump power required for transparency also increases. This is because $P_{thresh.}$ can be interpreted as the input pump power required to secure that the signal is not absorbed, up to transparency level. For a longer fiber, the transparency power must be higher, since the signal absorption is increased.
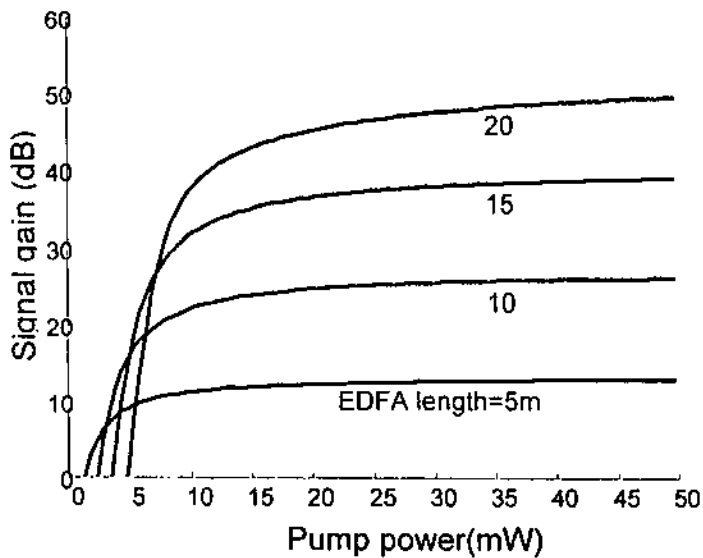


Figure 3.6 : Signal gain versus pump power, for different fiber lengths, calculated by numerical method for 1550 nm signal wavelength, for fiber A.

It may be useful here to introduce the effect of EDFA length on gain coefficient, which is defined as; the slope of the tangent to the curve gain as a function of pump power through the origin is by definition the EDFA gain coefficient, expressed in dB/mW units. This coefficient is a characteristic device parameter that should not be confused with the usual definition of amplifier gain factor, $\alpha_s$ derived earlier. A high gain coefficient corresponds to a steep increase of gain with pump power near the transparency value. It does not give an indication of the maximum EDFA gain or the

pump power required to achieve a given level; instead it reflects how rapidly the gain gets to its maximum value, as illustrated in Figure (3.6) as the length increases the gain coefficient increases.

## 3.4.2 Signal Gain Versus EDFA Length

It is instructive here to plot both the pump and signal power evolution as a function of position. For 50m length of fiber A, launched with different pump power. Using the simulation engine described earlier, considering copropagating signal and pump. The signal initiated power was assumed to be 0.1 µW, at 1550 nm wavelength. The result is shown in Figure (3.7). The following points are clearly noticed:

- The pump power will decay as it propagates along the EDFA, due to pump absorption, while the signal power will increase. The pump absorption is not rapid due to the finite emission cross section at 1480nm. When the pump is absorbed up to a reasonable level, the signal experiences gain.

- At certain length, the pump will be absorbed, so the signal power will reach its highest value. After that the signal will experience loss rather than gain. Arriving at this point will be faster for lower pump power.
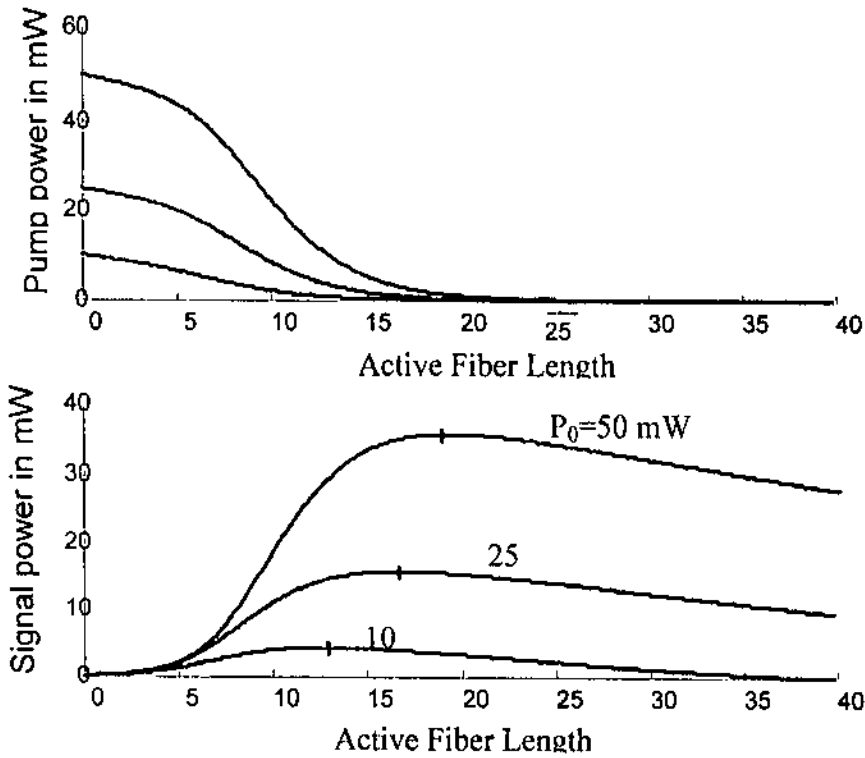
Figure 3.7:Signal and pump power evolution through fiber A of 40 m length. Indicating the maximum signal power reached

From Figure (3.7) power conversion efficiency (PCE) defined as

$$PCE = \frac{Psignal\_out - Psignal\_in}{P_{pump}}$$ (3.7)

For example PCE is about 70% for a pump power of 50 mW, while it is about 60% for 25 mW pump power. (i.e. power conversion efficiency increases with pump power increase).

From the previous result, and knowing that the signal gain is governed by the population inversion, it is obvious to plot the signal gain in fiber A for two input pump powers, 10 mW and 40 mW, and for two signal wavelengths 1530 nm and 1550 nm with initial signal power of 0.1 μW. The result of such simulation is shown in Figure (3.8) and (3.9), which confirm our previous observation; that is the signal will die at shorter distance for lower pump power for both wavelengths. The attractive notice here

is that the attenuation in the signal is slower for 1550nm wavelength due to its flattened
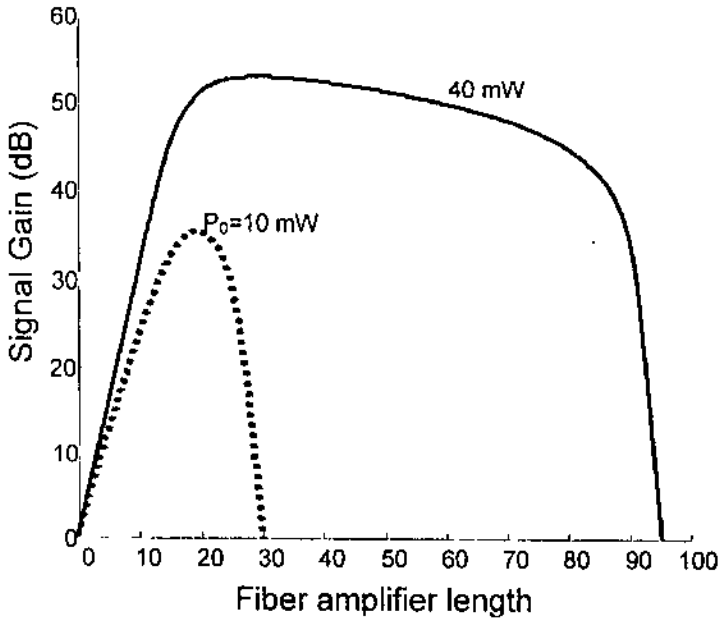
spectrum described earlier.



**Figure 3.8 : Signal gain at 1530 nm for 1480 nm pumping of fiber A, as a function of fiber length. The launched pump power is 10 mW (dotted), and 40 mW (solid).**
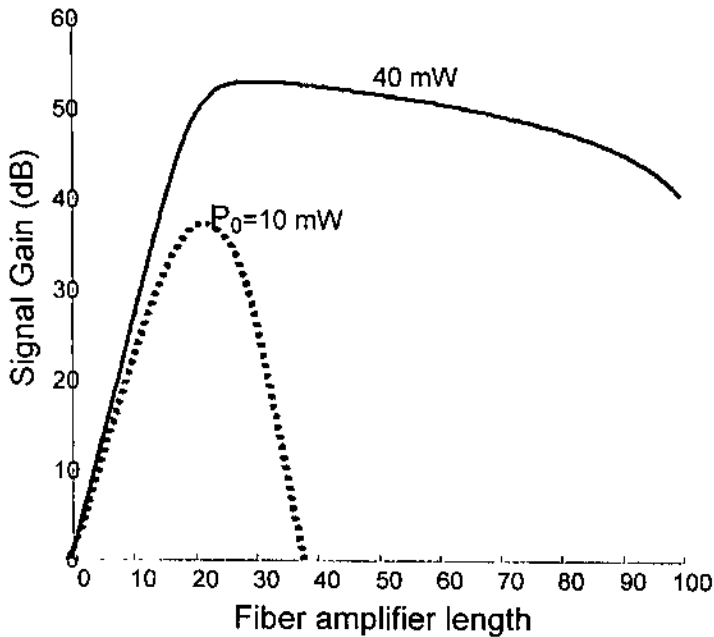


**Figure 3.9 : Signal gain at 1550 nm for 1480 nm pumping of fiber A, as a function of fiber length. The launched pump power is 10 mW (dotted), and 40 mW (solid).**

. The most important feature of these results is the existence of an optimum length

different for each input pump power, for which the signal gain is maximized. For a

given pump power, to obtain the maximum amount of gain for a given erbium concentration in the fiber core, the fiber length should be increase until maximum gain is obtained, then the gain will drop down again. Figure (3.10) shows the optimum length plotted as a function of pump power for two input signal, one small signal power, -40 dBm, and moderate signal power , -15 dBm
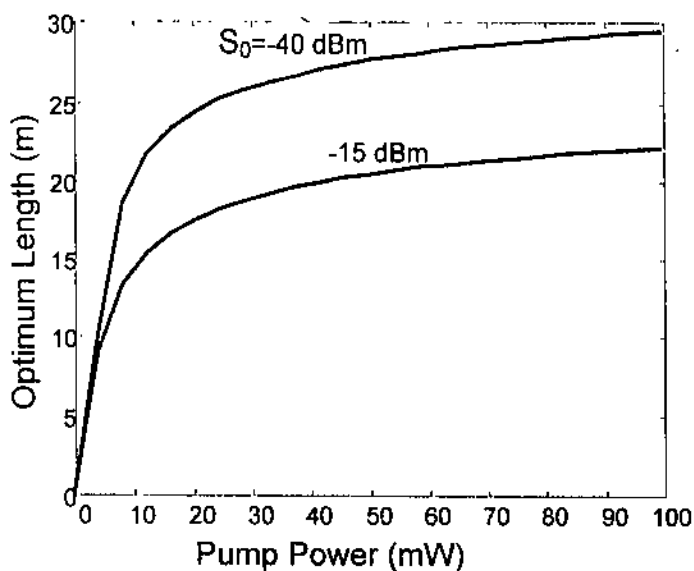


Figure 3.10: Optimum length versus pump power

It is obvious that as the pump power increases longer EDFA is needed. It can be noticed also that the optimum length increases for lower input signal power, since as expected lower input signal power yields higher gain and accordingly need longer fiber.

## 3.4.3 Signal Gain Versus Erbium Profile

Considering first the step-like profile for erbium concentration $N_0(r)$

$$N_0(r) = \begin{cases} No & r \le a_d \\ 0 & r > a_d \end{cases}$$

Where "$a_d$" is the doping radius. This profile is shown in Figure 3.11, together with the signal and pump mode profiles that are plotted as function of the radial distance from the center of the fiber. The transverse mode profiles were computed from the Bessel function solution for a single-mode step index fiber as discussed earlier.
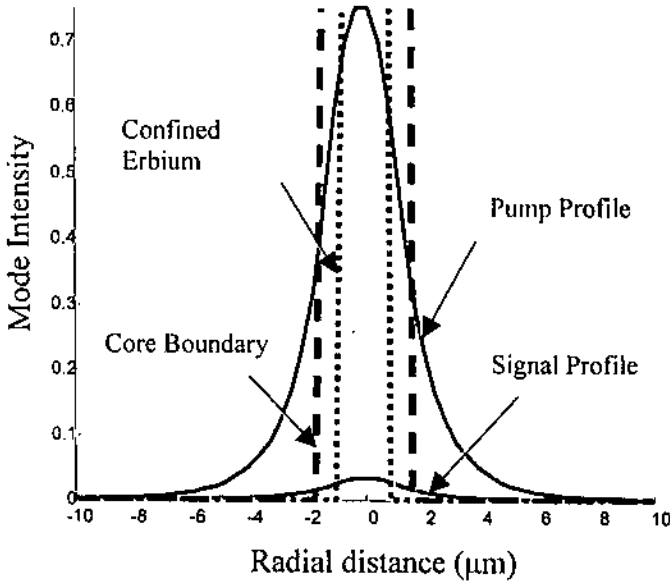


Figure 3.11: Transverse mode profiles for signal and pump, together with erbium concentration profile

The effective volume occupied by the pump and signal modes and their overlap with the region containing the active medium, plays an important role in determining the gain factor, $\alpha'_s$. The effect of erbium confinement is illustrated in Figure (3.12) where the gain is plotted as a function of pump power for a given length. Two fibers were used in the simulation; one with no erbium confinement (erbium uniformly distributed throughout the core), and one with erbium confined within the core to cylinder of radius

50% of core radius. The signal wavelength is 1550nm with a launched signal power of 0.1μW in the fiber A. Here also there are different arguments that can be noted regarding the power regions. Clearly, confining the erbium to a region with a radius one-half that of the core radius results in an increase in the gain efficiency for low pump powers. For high pump powers, the confined fiber results in a decrease in the gain. This happens due to the fact that population inversion will be easier to obtain in the region where the pump intensity is the strongest.
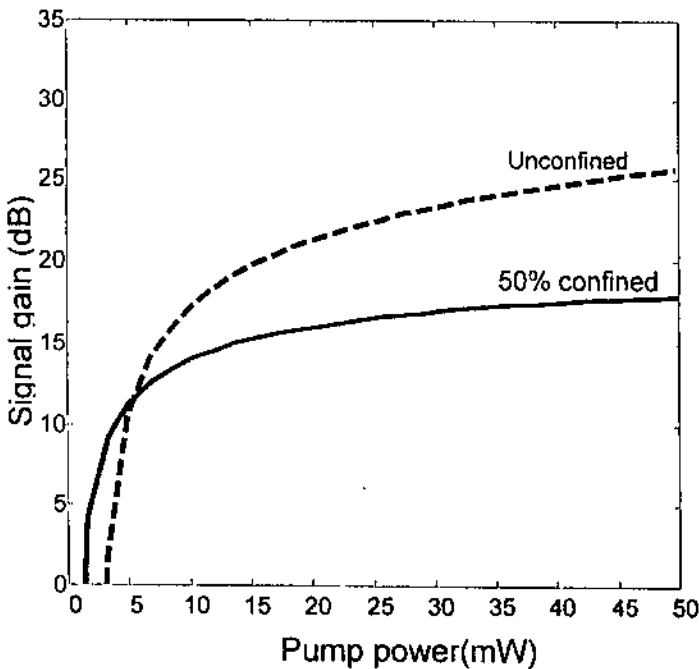
**Figure 3.12: Signal Gain as function of pump power, for 50% confined erbium concentration , (solid), and 100% unconfined erbium concentration profile (dashed), both of 12 m length.**

To get benefit from the high efficiency at low pump powers, while maintaining the high gain at the high pump powers region, the confined fiber should be made longer than that unconfined one. This is illustrated in Figure (3.13) where the gain is plotted against pump power for two fibers; one with 50% radius confinement with length of 30 m, the other is uniformly distributed with length 12 m. For confined fiber higher gain efficiency is obtained in the low pump regime, while, there is no difference in the overall gain for high pump powers.
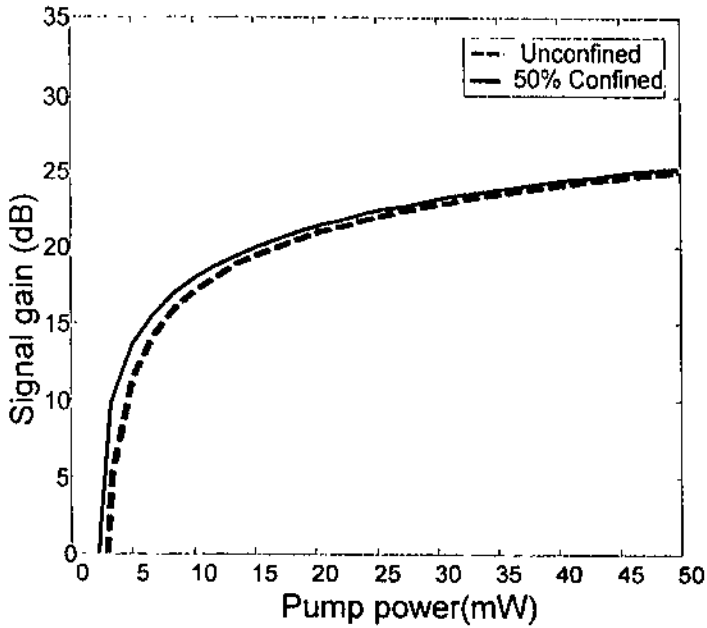
Figure 3.13: Signal Gain as function of pump power, for 50% confined erbium concentration , (solid) of 30 m length, and 100% unconfined erbium concentration profile (dashed) of 12 m length.

Figure (3.14) shows typical signal gain as a function of $Er^{3+}$ doped fiber length for unconfined and 50% confined erbium concentration. The simulation is performed at input signal power of 0.1μW at 1550nm. The pump power used was 40mW.

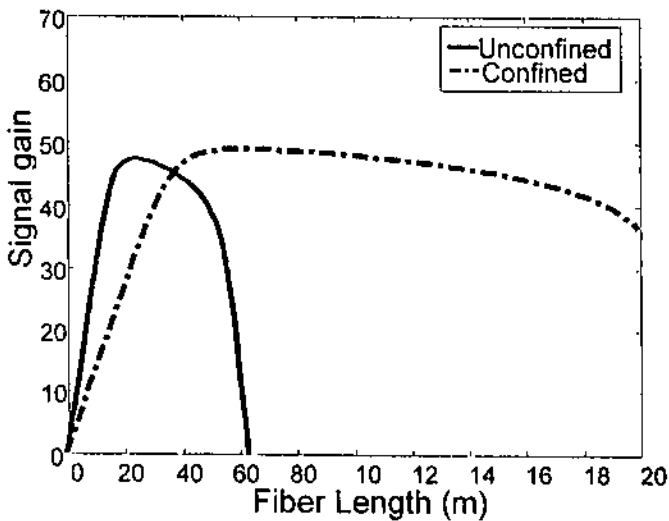The main disadvantage of confinement structure is that it requires longer EDFA.



Figure 3.14: Signal Gain as function of EDFA length, once for 50% confined erbium concentration , (dashed) , and 100% unconfined erbium concentration profile (solid), both at pump power of 40mW, at 1480 nm pump wavelength, and 1550 nm signal of power 0.1 μm .

Secondly, consider gaussian erbium concentration profile as shown in Figure (3.15). As known, the single-mode is approximated by guassian function expressed as

$E_g = E_0\, e^{-r^2/r_0^2}\, e^{-j\beta z}$, where $r_0$, the mode field radius, approximated by $\dfrac{a}{\sqrt{\ln V}}$. So the erbium concentration profile was chosen such that $Er\_conc = 0.7 x 10^{25}\, x e^{-r^2/r_0^2}$
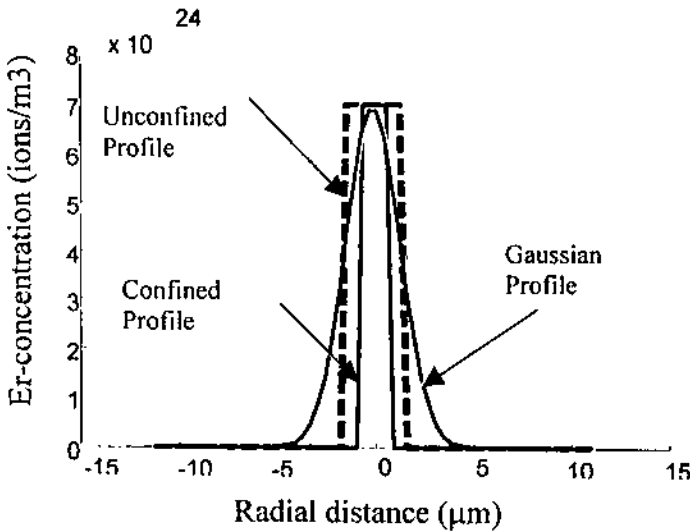


**Figure (3.15): Er-concentration profiles**

It is clear from Figure (3.16) that the gaussian profile has very similar effect on signal gain as that of the unconfined fiber in the small power region.
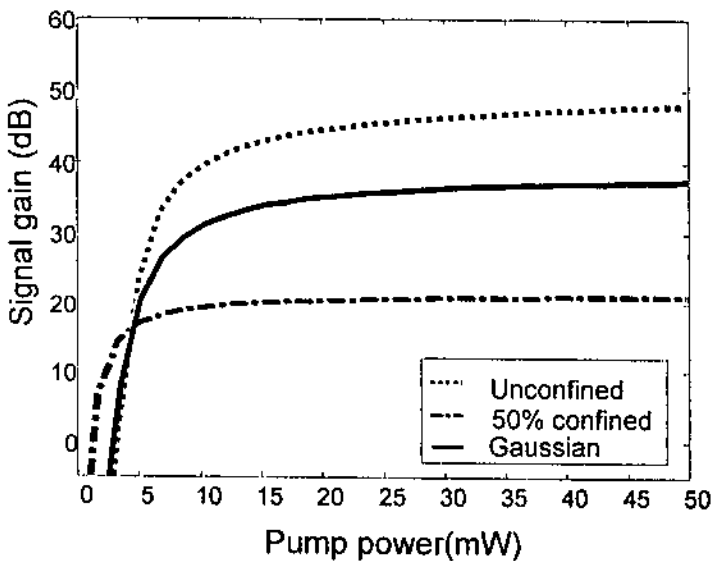


**Figure 3.16: Signal Gain as function pump power, once for 50% confined erbium concentration , (dashed) , unconfined erbium concentration (dotted), and guassian profile concentration (solid), all at 1550 nm signal of power 0.1 um, and fiber length of 14 m .**

In the higher power region, where the gain is approximately constant, the gaussian profile provides smaller gain than the unconfined but more than the confined. A fiber of 14m length was used.

This decrease in gain would be compensated by increasing the length of EDFA. This result is illustrated in Figure (3.17) shown below.
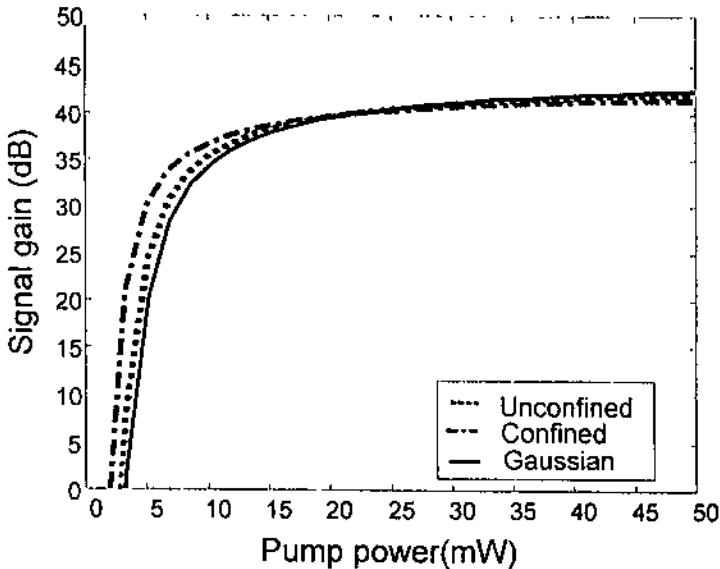


Figure 3.17: Signal Gain as function pump power, once for 50% confined erbium concentration, 28 m (dashed), unconfined erbium concentration, 12 m (dotted), and guassian profile concentration, 16 m (solid), all at 1550 nm signal of power 0.1 um.

The maximum signal gain depends strongly on the $Er^{3+}$ concentration. This is illustrated in Figure (3.18). In this simulation fixed length of 14m was used, the erbium concentration was assumed to be uniformly distributed across the core radius, with concentration of $qx0.7x10^{25}$ ions/m$^3$, where q is taken to be one of the following consequently {0.1, 0.5, 1, 2, 5, 10, 15}
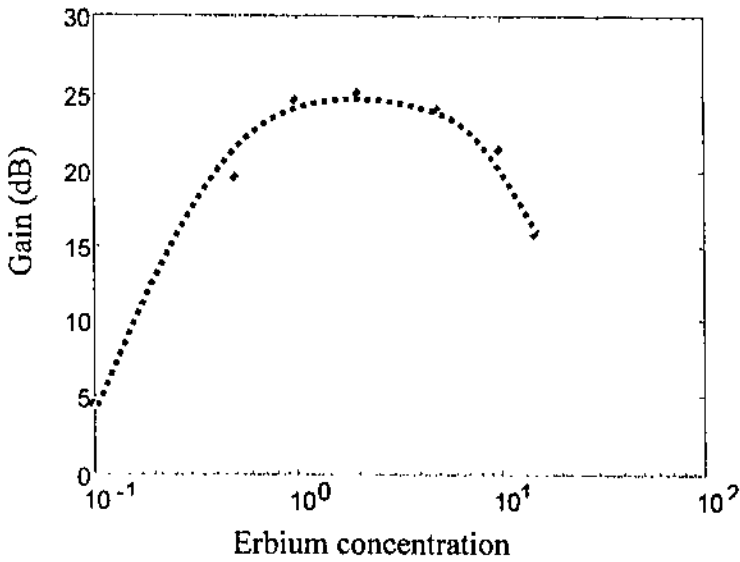
**Figure 3.18:** Signal Gain as function erbium concentration, the original erbium concentration is $0.7 \times 10^{25}$ ions/m³, multiplied by ( 0.1, 0.5, 1, 2, 5, 10,15).

As shown in Figure (3.18), as the erbium concentration increases, the gain increases accordingly, until the gain reaches to its maximum, then it drops again regardless to any raise in concentration. This happens due to what is called $Er^{3+}$- $Er^{3+}$ interaction effects (Desurvire,1994). Ideally speaking, the ions of erbium are independent, that is if one ion is excited to the $I^4_{13/2}$ state doesn't prevent a neighboring ion from also being excited to $I^4_{13/2}$ state. Actually this is not the case when the concentration of erbium is increased to certain extend where the ions' excitation becomes dependant on other ions.

*520924*

### 3.4.4 Signal Gain Versus Forward and Backward Propagation

According to pumping configurations illustrated in Figure (1.5), the effect of forward and backward pumping are demonstrated in Figure (3.19) shown below.
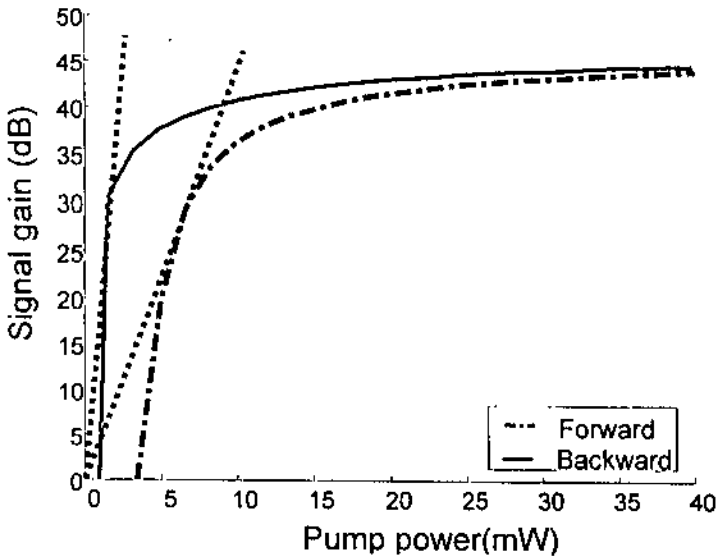


**Figure 3.19:** Signal Gain as function pump power, for forward pumping (dashed), and backward pumping (dotted). Both at pump wavelength 1480 nm.

Backward pumping would result lower threshold and higher efficiency and higher maximum gain in the low pumping power region. At high pump power region, it makes no difference if EDFA was pumped backward or forward. The reason that the backward pump is more efficient than forward is that in the backward pump propagation case the pump is strongest in the region where the signal is strongest. That is; in the copropagating configuration the portion of the fiber that the signal enters tends to be more inverted than the section by which the signal exits. Thus the signal undergoes more gain per unit length at the beginning of the fiber than at the exit. In the counterpropagating configuration, the inverse situation is present, and the lower gain per unit length at the beginning of the fiber is equivalent to have some amount of loss for the signal before it enters the amplifier. For high pump power, the pump will

strongly invert the entire fiber and it will not matter whether the pump is copropagating or counterpropagating.

## 3.4.5 Signal Gain Versus Numerical Aperture (NA)

The effect of the transverse design is also illustrated by changing the numerical aperture and thus the pump and signal intensities, and their overlap with each other as well as with the Erbium distribution. At low pump power region, the advantage of the high NA fiber with its reduced core and mode field diameters is quite clear. It provides better efficiency and smaller pump power threshold.
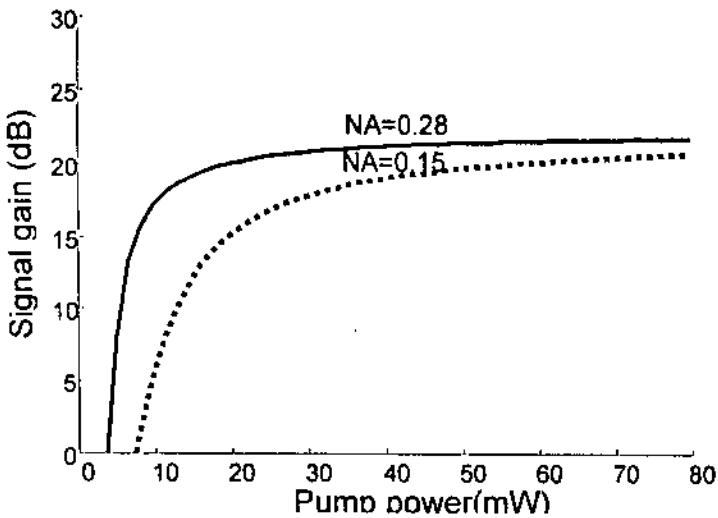


Figure 3.20: Gain for a relatively high NA fiber (NA =0.28, a=1.4μm) and a low NA fiber (NA=0.15, a=2.0 μm), as a function of pump power at 1480 nm of 14 m length, and Er$^{3+}$ is uniformly distributed across the core.

This advantage is removed at higher pump powers where both fibers are well inverted and the low NA fiber achieves high gains. This is shown clearly in Figure (3.20) where two fibers were used, one with high NA=0.28, core radius 1.4μm, and the other with NA=0.15, core radius 2.0μm. the signal power 0.1μW at 1550nm, 14m length, and uniformly distributed erbium across the core.

## 3.5 Basic Characteristics

The basic amplification characteristics, such as the signal gain characteristics, gain spectrum, and saturation characteristics are investigated in the coming subsections.

### 3.5.1 Signal Gain Dependency on Signal Power

From the discussion in the previous subsection, signal gain and gain coefficient (efficiency) depends highly on fiber length, pump power, signal wavelength, $Er^{3+}$ concentration and EDFA structure.
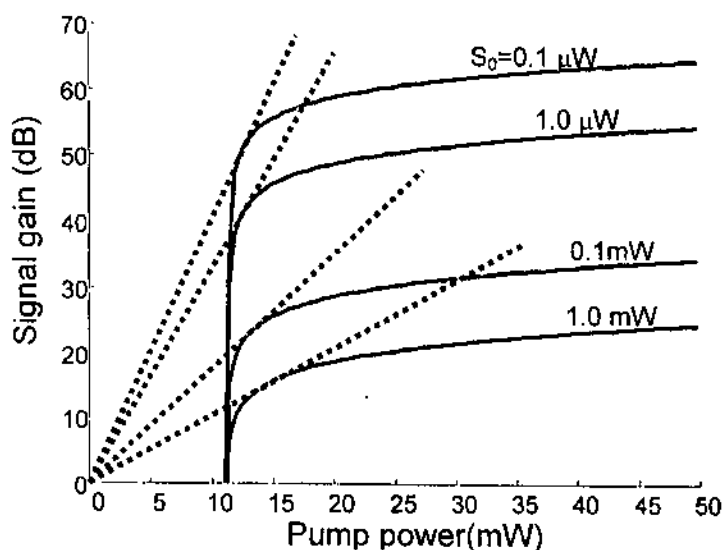


**Figure 3.21: Gain versus pump power for several signal power**

Moreover, it is shown here that they also depend on input signal power; such that as the input power increases the gain decreases and efficiency also decreases. This fact is illustrated in Figure (3.21), in this Figure the signal gain is plotted as function of pump power, for different input signal power all at 1550 nm, and fixed length of fiber A (14m). The pump wavelength is 1480 nm.

## 3.5.2 Gain Spectrum

Simulation also can predict the gain as a function of wavelength. Since the radius of the absorption and emission cross sections differ from wavelength to another, the spectral shape of gain will be as that shown in Figure (3.22) shown below.
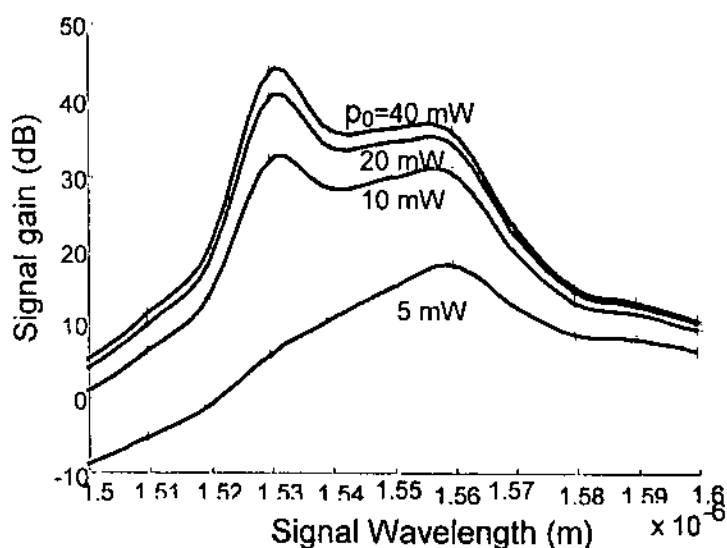


Figure 3.22: Gain versus signal wavelength for several pump power

The gain as a function of signal wavelength is plotted for input signal power of 0.1 μW for the pump powers, 5, 10, 20, and 40 mW, for a 14 m length of EDFA fiber A. It is noticeable that the gain change nonuniformly with changes in pump power. In particular, as pump power decrease, signals near 1530nm will suffer a drop in gain much more significant than signals near 1550nm.

## 3.5.3 Saturation Characteristics

Gain saturation (defined as the output power at which the gain is compressed from its small gain value by 3 dB (Sudo,1997)) can also be modeled. Figure (3.23) shows the gain as a function of output signal power in a 14m length of fiber A. The signal wavelength is 1550nm, and the three pumping powers are 15, 40, and 65mW at a pump wavelength of 1480nm.



**Figure 3.23: Signal Gain as function of output signal power for different pump powers (15, 40 and 65 mW)**

As the signal power increases past the small signal value, the gain decreases since the pump can no longer replenish the inversion as fast as the signal depletes it. The small signal gain and the saturation output power both increase with pump power.

# CHAPTER (4):Recommendations and Applications
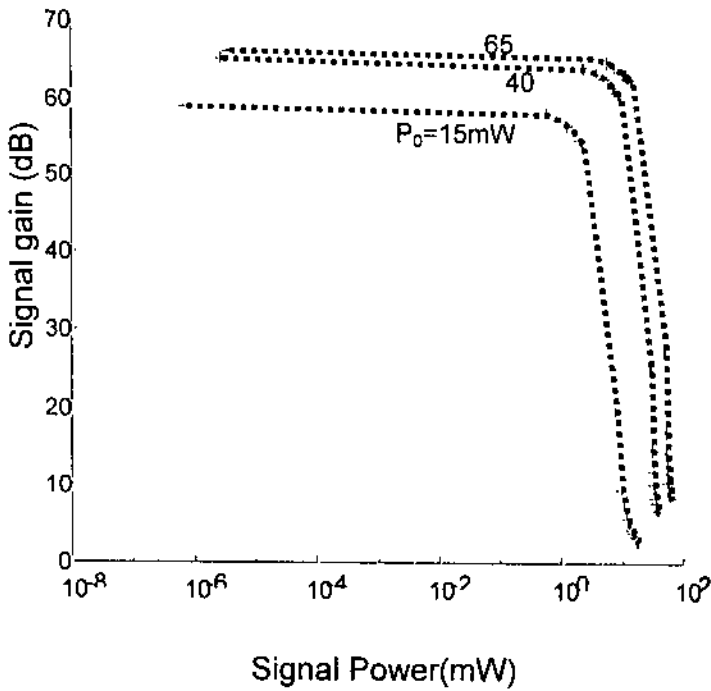
## 4.1 Conclusion

Throughout this work, one can clearly notice some of the many advantages of the erbium doped fiber amplifiers, such as:

- They provide high gain (30-50 dB).

- They provide high conversion efficiency (40-70%).

- They can easily be integrated in a fiber network, since they are already silica-based fiber components.

- The saturation characteristics are very good, because the saturation power can be linearity increased with the pump power.

- They operate in the range of 1.5-1.6 $\mu$m, which coincides with the low-loss region in silica-based fibers.

- They are transparent to bit rate and waveguide. This facilitates system upgrading and reconfiguration.

The main parameters in the design of EDFA, include the fiber glass material, the waveguide characteristics of the fiber, the $Er^{3+}$ concentration profile, the length of fiber used, the pump source,...etc. These parameters need to be considerable as a whole when designing an amplifier for various applications, taking into consideration the manufacturing constrains of the fiber.

Maximizing the gain is the most important issue under concern here, since it is considered as the main requirement in almost all applications. Some keys that yield achieving high gain in EDFA will be discussed here below:

(1) . *High optical intensity in the core:*

Which is obtained by reducing the mode field radius $r_0$, which by its turn depends on the core radius, $a$, and differential refractive index, $\Delta n$, ( or equivalently numerical aperture, $NA$,). As illustrated in section (3.3.5), where the gain is obviously higher for higher $NA$ with reduced core diameter, especially at low pump power. The increase in $NA$ and hence decrease in core radius, $a$, is limited, for the reason that background losses increase by $NA$ increase, and hence the gain degrades rather than improves. Also very small core radius cause more difficulty when connecting to standard fiber network, resulting in extra coupling losses.

(2) *Low loss fiber hosts:*

Such as silica-based glasses and fluoride-based glasses. In Silica-based glasses, transmission loss of 0.15 dB/km at 1.55 µm.

(3) *Efficient pumping in terms of pump power, and configuration:*

Higher pump power results in higher gain if suitable length was chosen, as was shown in sections (3.4.1) and (3.4.2). An important issue should be noted here; that is higher gain can be obtained by increasing the erbium doped fiber amplifier length at high pump powers. But sure losses would increase for very long EDFA, and thus degradation in gain will occur.

Regarding pumping configuration; forward and backward. As investigated in section (3.3.4), backward configuration yields significant higher gain especially when low pump power is used.

(4) . *A suitable erbium concentration:*

Step like erbium concentration profile $\begin{Bmatrix} N_0 & r \le a_d \\ 0 & r \ge a_d \end{Bmatrix}$ is the optimum concentration

profile. Where '$a_d$' is the doping radius. It is evident also that higher gain will be

obtained for $\dfrac{a_d}{a} < 1$ (i.e. confined concentration profile), if a suitable length is correctly

chosen. Maximum signal gain also can be achieved to be beyond $10^{25}$ ions/m$^3$ for '

optimum length of Ge/Al/Er-doped fiber. If other codopant other than Ge or Al were

used, the optimum concentration will change accordingly.

(5)　*Control of Er$^{3+}$ energy level lifetime by codoping:*

In addition to the fact that codoping is a necessary to improve Er$^{3+}$ solubility, and

increase gain bandwidth. Codoping material plays an important role in varying lifetime

and obtaining different emission and absorption cross sections, which results in

obtaining different gain. (Refer to section 3.2).

(6)　*An effective device configuration:*

Including isolators, filters, splicing and connectors, should all be of high quality to

ensure minimum loss.

## 4.2 Applications

In this section we focus on the keys issues recommended when designing EDFA for applications shown in Figure (1.3).

*In the case of preamplifiers*; usually the signal is small (e.g. -40dBm), very high gains are required, and a high efficiency fibers are needed if the pump power is not to be too high (e.g. ≤ 20mW). So it is advisable to use counterpropagating configuration and high NA (e.g. NA ≥ 0.3), since these conditions will improve the gain efficiency, and provide high gain.

*In the case of inline amplifiers*; with signal input levels in the -10 dBm to -20 dBm range. Quite often such amplifiers are required to have moderate gain. Pump powers are moderately high (e.g. on the order of 50 to 100 mW for long haul systems). In this case, moderate NA fibers (0.2 to 0.3) are suitable for such applications. It is very important for such applications that erbium doped fiber amplifiers have minimum losses. This can be achieved by avoiding long fibers or high NA fibers, for the reason that such fibers suffer from high background losses as previously mentioned.

*In the case of power amplifiers*; the signal range is relatively high (e.g 0 dBm), causing the amplifier to operate deep in saturation . The erbium doped fiber amplifier has an output saturation power that can be increased with pump power, as discussed in section (3.4.3). A high pump power can transfer a significant fraction of its energy to the signal, resulting in signal output that can reach several Watts. Operating in saturation, results that the gain is much flatter, as function of signal wavelength, than that of an amplifier operating in the small signal mode. This is illustrated clearly in Figure (4.1) shown below.
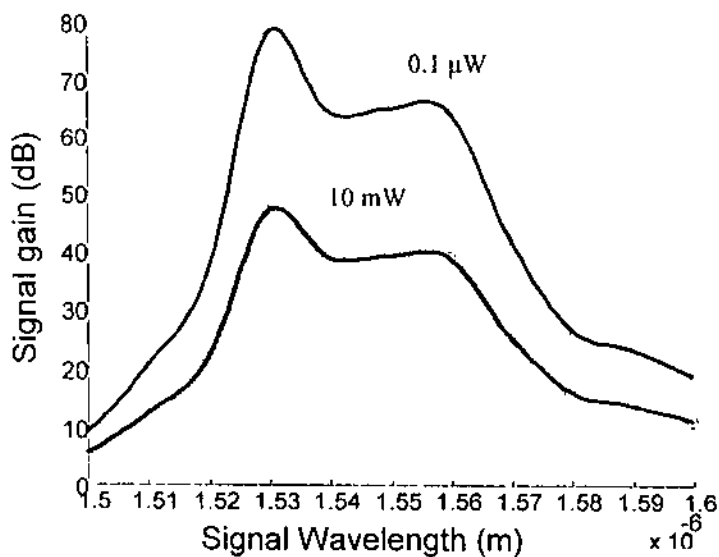
**Figure 4.1: Signal Gain versus signal wavelength for different input signal powers, 0.1μ W, and 10mW, for pump power 40 mW, and EDFA length of 20 m**
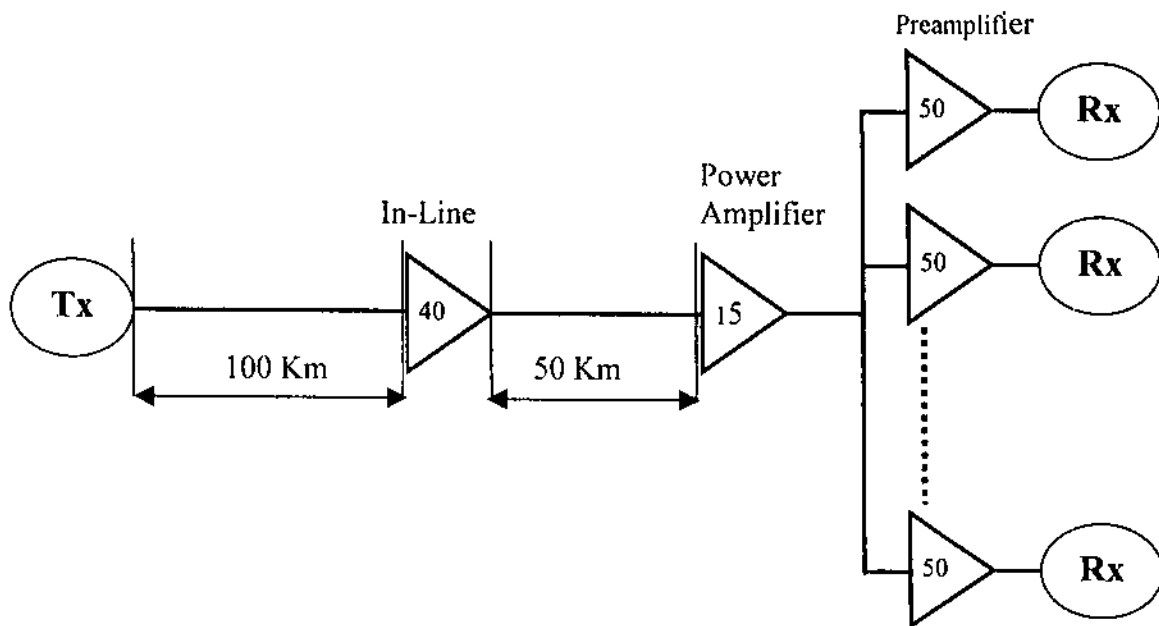


**Figure 4.2: Typical example showing amplifiers applications**

Figure (4.2) shows an example of how optical amplifiers are installed in real systems for different applications. We will assume a few things about the components available, all assumptions are all reasonable. Our assumptions include 5 dBm source output power, 3-dB source-fiber coupling loss, two connectors of 1 dB each, and 50 splices of 0.1 dB loss each. The splices are placed, on the average, every 2km along each path. We need them to simplify construction and installation of the fiber cable. Let's assume that we would like to transmit a video signal from location A, to location B, then distribute it to 1 million users using CATV (Common Antenna TV.). Then the power-budget calculations will be as summarized in Table (4.1) below. Taking into account the fiber attenuation to be 0.25dB/km.

**Table 4.1 : Power Budget Calculations**

| The first section | | |
|---|---|---|
| Laser diode output power | | 5 dBm |
| Source coupling loss | 3 dB | |
| Connector loss (2 connectors) | 2 dB | |
| Splice loss (50 splice) | 5 dB | |
| Fiber attenuation (100 km) | 25 dB | |
| Total loss | 35 dB | |
| Power available at inline amplifier | | -30 dBm |
| In line amplifier gain | 40 dB | |
| Power available after inline amplifier | | 10 dBm |
| **The second section** | | |
| Splice loss (25 splice) | 2.5 dB | |
| Fiber attenuation (50 km) | 12.5 dB | |
| Power available at the input of power amplifier | | -5 dBm |
| Power amplifier gain | 15 dB | |
| **The third section (branches)** | | |
| Power available after the power amplifier (at the input of the branches) | | 10 dBm |
| Power available at the input of preamplifier at each user (assuming 1 million users) | | -50 dBm |
| Preamplifier gain | 50 dB | |
| Power available at the input of each receiver | | 0 dBm |

## 4.3 Future Research topics

It has been shown how the EDFA comprises numerous advantages such as high gain, broad bandwidth, and high efficiency. In addition to their attractive characteristics of being transparent to both bit rate and wavelength. We expect that their use will continue to spread rapidly. Therefore, we list some suggested topics that constitute an integral part of this work.

- Studying the noise effect in EDFA due to Amplified Spontaneous Emission (ASE).

- Investigating the effect of the active element, $Er^{+3}$, on signal field profile and its evolution along the propagation axis.

- Studying pumping at different wavelengths, and treating the exact three-level energy system of $Er^{+3}$ ions instead of the simplified three systems. Moreover, studying the effect of excited state absorption (ESA) on amplifier performance.

- Studying planner optical amplifiers fabricated on optical integrated circuits.

- Including in the optimization and performance study of EDFA the effect of related components, such as isolators, beam couplers, splitters, splices, and pump sources.

- Performing some experimental work to compare with theoretical studies and models.

# References

□ Agrawal, G., 1997. Fiber-Optic Communication Systems, John Wiley & Sons. Inc.

□ Basch, E. E., 1986. Optical - Fiber Transmission, Howard W. Sams. & Co.

□ Becker, P., Olsson, N., and Simpson, J., 1999, Erbium-Doped Fiber Amplifiers: Fundamental and Technology, Academic Press.

□ Buck, J., 1995 Fundamentals of Optical Fibers, John Wiley & Sons. Inc.

□ Cummings, F., 1988, On Spontaneous Emission, IEEE . Quantum Electron., vol. 24, No. 7.

□ Derickson, D., 1998, Fiber Optic Test and Measurement, Prentice-Hall, Inc.

□ Desurvire, E., 1994, Erbium-Doped Fiber Amplifiers: principle and applications, John Wiley & Sons, Inc.

□ Dinand, M., and Sohler, W., 1994, Theoretical modeling of optical amplification in Er-doped Ti:LiNbO₃ waveguides, IEEE J. Quantum Electron., vol. 30, No. 5.

□ Gagliardi, R., and Karp, Sh., 1995, Optical Communication. John Wiley & Sons, Inc.

□ Giles, C., and Desurvire, E., 1991, Modeling Erbium-Doped Fiber Amplifiers, J. of Lightwave Technology, vol. 9, No. 2.

□ Kazovsky, L., Benedetto, S., and Willner, A.,1996, Optical Fiber Communication Systems, Artech House, Inc.

□ Lanchs, G., 1998, Fiber Optic Communications systems: analysis, and enhancements, McGraw-Hill.

□ Midwinter, J., and Gue, Y., 1992, Optoelectronics and Lightwave Technology, John Wiley & Sons, Inc.

□ Miniscalco, W., 1991, Erbium-Doped Glasses Fiber Amplifiers at 1500nm, J. of Lightwave Technology, vol. 9, No. 2.

❑ Ono,H., Yamada, M., Kanamori, T., Sudo, S., and Ohishi, Y., 1999, 1.58-µm Band Gain-Flattened Erbium-Doped Fiber Amplifiers for WDM Transmission Systems, J. of Lightwave Technology, vol. 17, No. 3.

❑ Palais, J., 1998, Fiber Optic Communications, Prentice-Hall, Inc.

❑ Pedersen, B., Bjarklev, A., Povlsen, J., Dybdal, K., and Larsen, C., 1991, The Design of Erbium-Doped Fiber Amplifiers, Journal of Lightwave Technology, vol. 9, No. 9.

❑ Senior, J., 1992, Optical Fiber Communications Principles and Practice, Prentice-Hall, Inc.

❑ Shimada, S., and Ishio, H., 1994, Optical Amplifiers and their Applications, John Wiley & Sons Ltd.

❑ Sudo, S., 1997, Optical Fiber Amplifiers, Artech House, Inc.

ملخص


## نَمذجة وتحليل أداء والأمثلة لمضخم ضوئي مضافاً إليه عنصر الإربيوم


إعداد

رتا أحمد رمضان


إشراف

د. إبراهيم منصور


مع اتساع رقعة استخدام الاتصالات الضوئية خاصة لإرسال معلومات بسرعات عالية لمسافات طويلة، فقد ازدادت الحاجة لاستخدام المضخات. وقد وُجد أن المضخمات الضوئية تلقى وبشكل ملحوظ بديلاتها من المضخمات الإلكترونية حيث أنها لا تعتمد على سرعة المعلومات أو طول الموجة الناقلة لها.

تعتبر المضخمات الضوئية المضاف إليها عنصر الإربيوم من أهم المجالات التي اجتذبت اهتمام الباحثين في مجال الاتصالات الضوئية، حيث أنها أثبتت كفاءة عالية في أدائها.

لقد حاولنا من خلال هذا العمل القيام بتحليل نظري ورياضي بصف أسلوب عمل هذه المضخمات. ومن خلاله دراسة أدائها، آخذين بعين الاعتبار المتغيرات التي تؤثر على أدائها مثل: طول الليف الضوئي النشيط، تركيز وشكل توزيع مادة الإربيوم، أبعاد المقطع العرضي لليف الضوئي وتركيبه الليزيتي، بالإضافة إلى قدرة المضخة وكذلك قوة الإشارة الضوئية. وفي النهاية تمّ وضع التوصيات اللازمة للحصول على أعلى نسبة كسب ممكنة من خلال أمثلة المتغيرات أعلاه.